Synthesis and Characterization of Rhenium Thiolate Complexes. Crystal and Molecular Structures of $[NBu_4][ReO(H_2O)Br_4)]\cdot 2H_2O$, $[Bu_4N][ReOBr_4(OPPh_3)]$, $[ReO(SC_5H_4N)_3]$, $[ReO(SC_4H_3N_2)_3][ReO(OH)(SC_5H_4N\text{-}3,6\text{-}(SiMe_2Bu^t)_2)_2]$, $[Re(N_2COC_6H_5)(SC_5H_4N)Cl(PPh_3)_2]$, and $[Re(PPh_3)(SC_4H_3N_2)_3]$

David J. Rose,[†] Kevin P. Maresca,[†] Peter B. Kettler,[†] Yuan Da Chang,[†] Victoria Soghomomian,[†] Qin Chen,[†] Michael J. Abrams,[‡] Scott K. Larsen,[‡] and Jon Zubieta*,[†]

Department of Chemistry, Syracuse University, Syracuse, New York 13244-4100, and Johnson-Matthey, Metallopharmaceutical Research, 1401 King Road, West Chester, Pennsylvania 19380

Received July 13, 1995[⊗]

The syntheses and characterizations of six monomeric rhenium thiolate complexes and the structural characterization of two useful rhenium starting materials are presented. Pyridine-2-thiol (**1**) and its derivatives 3-(trimethylsilyl)-pyridine-2-thiol (**2**), 3,6-bis(dimethyl-*tert*-butylsilyl)pyridine-2-thiol (**3**), and pyrimidine-2-thiol (**4**) were reacted with $[Bu_4N][ReOBr_4(H_2O)]\cdot 2H_2O$ (**5**), $[Bu_4N][ReOBr_4(OPPh_3)]$ (**6**), $[ReO_2(C_5H_5N)_4]$, and $[Re\{N_2CO(C_6H_5)\}Cl_2(PPh_3)_2]$ to give $[ReO(C_5H_4NS)_3]$ (**7**), $[ReO(C_8H_{12}NSiS)_3]$ (**8**), $[ReO(OH)(C_{11}H_{20}NSi_2S)_2]$ (**9**), $[Re\{N_2CO(C_6H_5)\}Cl(PPh_3)_2(C_5H_4NS)]$ (**10**), $[ReO(C_4H_3N_2S)_3]$ (**11**), and $[Re\{P(C_6H_5)_3\}(C_4H_3N_2S)_3]$ (**12**). Crystal data: **5**, $C_{16}H_{42}NO_4Br_4Re$, tetragonal, $I\bar{4}$, $a = 8.779(2)$ Å, $b = 11.614(2)$ Å, $c = 9.397(2)$ Å, $\beta = 114.67(3)°$, $V = 870.7(4)$ Å^3, $Z = 2$, 422 reflections, $R = 0.0457$; **6**, $C_{34}H_{51}NO_2PBr_4Re$, triclinic, $P\bar{1}$, $a = 14.437(3)$ Å, $b = 16.589(3)$ Å, $c = 16.783(3)$ Å, $\alpha = 94.87(3)°$, $\beta = 97.62(3)°$, $\gamma = 93.80(3)°$, $V = 3957(2)$ Å^3, $Z = 4$, 6141 reflections, $R = 0.0758$; **7**, $C_{15}H_{12}N_3OS_3Re$, monoclinic, $P2_1/c$, $a = 11.533(2)$ Å, $b = 11.385(2)$ Å, $c = 14.039(3)$ Å, $\beta = 107.97(3)°$, $V = 1749.8(9)$ Å^3, $Z = 4$, 1869 reflections, $R = 0.0322$; **9**, $C_{34}H_{65}N_2O_2S_2Si_4Re$, triclinic, $P\bar{1}$, $a = 8.072(2)$ Å, $b = 11.409(2)$ Å, $c = 12.402(3)$ Å, $\alpha = 79.67(3)°$, $\beta = 74.05(3)°$, $\gamma = 86.18(3)°$, $V = 1080.2(5)$ Å^3, $Z = 1$, 4630 reflections, $R = 0.0525$; **10**, $C_{48}H_{39}N_3OSP_2ClRe$, triclinic, $P\bar{1}$, $a = 10.842(2)$ Å, $b = 13.660$ (3) Å, $c = 17.665(4)$ Å, $\alpha = 86.37(3)°$, $\beta = 89.93(3)°$, $\gamma = 77.22(3)°$, $V = 2080.2(10)$ Å^3, $Z = 2$, 4329 reflections, $R = 0.0437$; **11**, $C_{12}H_9N_6OS_3Re$, orthorhombic, *Pbca*, $a = 8.240(2)$ Å, $b = 13.373(3)$ Å, $c = 29.388(6)$ Å, $V = 3238.4(16)$ Å^3, $Z = 8$, 1400 reflections, $R = 0.0512$; **12**, $C_{31}H_{26}N_6S_3PCl_2Re$, triclinic, $P\bar{1}$, $a = 9.224(2)$ Å, $b = 12.050(2)$ Å, $c = 17.665(4)$ Å, $\alpha = 89.25(3)°$, $\beta = 85.70(3)°$, $\gamma = 67.94(3)°$, $V = 1604.0(8)$ Å^3, $Z = 2$, 3592 reflections, $R = 0.0697$.

Introduction

Over the past 15−20 years, the chemistry of technetium and rhenium has expanded dramatically due to the utilization of their radionuclides either as diagnostic imaging agents (^{99m}Tc) or as combined diagnostic/therapeutic (^{186,188}Re) radiopharmaceuticals.[1−10] The ^{99m}Tc radionuclide has several advantages over other radionuclides which include cost, availability, and low-radiation-absorbed dose. These advantages are in part manifested by the nuclear properties of ^{99m}Tc ($t_{1/2} = 6.02$ h; $\gamma = 140.6$ keV) which also enable imaging results to be applied to clinical evaluation quite rapidly. Consequently, ^{99m}Tc imaging agents have been developed that are highly successful in imaging various anatomical features such as the brain, heart, lung, bone, GI tract and kidneys.[1−5]

More recently, radiopharmaceuticals utilizing rhenium, the group VIIB congener of technetium, in the form of the radioisotopes ^{186}Re and ^{188}Re have been developed.[6−10] The nuclear properties of ^{186}Re are particularly attractive because of its half-life (90 h) and strong β emission ($\beta_{max} = 1070$ keV) which enable this isotope to deliver high-radiation doses to tissues. Also, ^{186}Re has a photon emission at approximately the same energy as ^{99m}Tc ($\gamma = 137$ keV), allowing the radioisotope to be imaged by γ cameras utilized in conventional ^{99m}Tc diagnostic imaging. A rhenium radiopharmaceutical, ^{186}Re(Sn)HEDP, has been developed for the palliation of painful osseus metastases.[10,11]

The periodic relationship between technetium and rhenium suggests that therapeutic rhenium radiopharmaceuticals can be designed by analogy to existing ^{99m}Tc diagnostic agents.

[†] Syracuse University.
[‡] Johnson-Matthey.
[⊗] Abstract published in *Advance ACS Abstracts,* May 1, 1996.

(1) Pinkerton, T. C.; Desilets, C. P.; Hoch, D. J.; Mikelsons, M. V.; Wilson, G. M, *J. Chem. Educ.* **1985**, *62*, 965.
(2) Clarke, M. J.; Podbielski, L. *Coord. Chem. Rev.* **1987**, *78*, 253.
(3) Steigman, J.; Echelman, W. C. The Chemisty of Technetium in Medicine, Nuclear Science Publication NAS-NS-301; National Academy Press: Washington, DC, 1992.
(4) Deutsch, E.; Libson, K.; Jurisson, S.; Lindoy, L. F. *Progr. Inorg. Chem.* **1983**, *30*, 75.
(5) Jurisson, S.; Desilets, C. P.; Jia, W.; Ma, D. *Chem. Rev.* **1993**, *93*, 1137.
(6) Deutsch, E.; Libson, K.; Vanderheyden, J.-L.; Ketring, A. R.; Maxon, H. P. *Nucl. Med. Biol.* **1986**, *13*, 465.
(7) Ehrhardt, J.; Ketring, A. R.; Turpin, T. A.; Razavi, M.-S.; Vanderheyden, J.-L.; Su, F.-M.; Fritzberg, A. R. In *Technetium and Rhenium in Chemistry and Nuclear Medicine 3*; Nicollini, M., Bandoli, G., Mazzi, U., Eds.; Cortina International: Verona, Italy, 1990; p 631.
(8) Häfeli, U.; Tiefenance, L.; Schuberger, P. A. In ref 7, p 643.
(9) Nosco, D. L.; Tofe, A. J.; Dunn, T. J.; Lyle, L. R.; Wolfangel, R. G.; Bushman, M. J.; Grummon, G. D.; Helling, D. E.; Marmion, M. E.; Milles, K. M.; Pipes, D. W.; Saubel, T. W.; Webster, D. W. In ref 7, p 381.
(10) Maxon, H. R., III; Schroder, L. E.; Thomas, S. R.; Hertzberg, V. S.; Deutsch, E.; Samotunga, R. C.; Libson, K.; Williams, C. C.; Maulton, J. S.; Schneider, H. J. In ref 7, p 733.
(11) Vanderheyden, J.-L.; Heeg, M. J.; Deutsch, E. *Inorg. Chem.* **1988**, *27*, 1666.

S0020-1669(95)00881-0 CCC: $12.00

Therefore, it is anticipated that ^{99m}Tc diagnostic agents which accumulate in abnormal tissue may be used to model the development of ^{186,188}Re analogues with similar biodistribution properties.[6]

One approach in targeting radiopharmaceutical delivery systems exploits what is termed the "metal-tagged" approach.[5,12] Specifically, the covalent attachment of a radionuclide to an antibody by a bifunctional chelate has been utilized for diagnostic oncological applications and also for imaging focal sites of infection.[13] Recently, we explored the coordination chemistry of technetium organohydrazine complexes to model the uptake of ^{99m}Tc by a bifunctional hydrazine reagent.[14−18] Technetium(V) oxo precursors were found to add readily under mild conditions to hydrazinopyridine-modified proteins to yield stable ^{99m}Tc-labeled proteins in >90% radiometric yield.[19] Technetium-99m hydrazinopyridine−polyclonal IgG conjugates have been demonstrated to be useful agents for the imaging of focal sites of infection.[20]

Concurrent with the development of new bifunctional chelates is the development of new coligands that will aid in the stabilization of such bifunctional chelates. As we have observed earlier, the identity of coligands may profoundly influence the structures adopted by complexes possessing [MNNR] or [MN-NR_2] cores.[14−28] Coligands containing sulfur donor atoms have been particularly effective in the isolation and characterization of these complexes as a consequence of the high affinity of technetium and rhenium for sulfur ligands. To this end, we have decided to investigate the reactivity of pyridine-2-thiol (**1**), sterically hindered pyridine-thiols (**2**, **3**), and pyrimidine-2-thiol (**4**) as coligands for the study of antibody-labeling of radionuclides. While pyridine-2-thiol is a ubiquitous ligand that has been coordinated to almost all metals in the periodic table,[29−34] its functionalization with bulky triorganosilyl groups at either the 3- or the 6-position of the pyridine ring to form sterically hindered pyridinethiols and the subsequent reactivity studies of these ligands with a variety of transition metals have only been reported recently.[35−40] Previously reported reactivity studies with sterically hindered pyridinethiols have been performed primarily with late transition metals and molybdenum. Also, the reactivity of **1** toward rhenium has been limited in scope to only low-valent rhenium carbonyl complexes and clusters.[41−43]

Herein, we report reactivity studies for **1** and for the sterically hindered pyridinethiol ligands 3-(trimethylsilyl)pyridine-2-thiol (**2**), 3,6-bis(*tert*-butyldimethylsilyl)pyridine-2-thiol (**3**), and pyrimidine-2-thiol (**4**) with the high-valent rhenium precursors $[Bu_4N][ReOBr_4(H_2O)]\cdot 2H_2O$ (**5**), $[Bu_4N][ReOBr_4(OPPh_3)]$ (**6**), $[ReO_2(py)_4]$, and $[Re\{N_2CO(C_6H_5)\}Cl_2(PPh_3)_2]$. The resulting pyridine thiolate derivatives, $[ReO(\eta^2\text{-}2\text{-}SC_5H_4N)_2(\eta^1\text{-}2\text{-}SC_5H_4N)]$ (**7**), $[ReO(\eta^2\text{-}2\text{-}SC_5H_3N\text{-}3\text{-}SiMe_3)_2(\eta^1\text{-}2\text{-}SC_5H_4N\text{-}3\text{-}SiMe_3)]$ (**8**), $[ReO(OH)(\eta^2\text{-}2\text{-}SC_5H_2N\text{-}3,6\text{-}(SiMe_2Bu^t)_2)]$ (**9**), $[Re(\eta^1\text{-}N_2CO(C_6H_5))(\eta^2\text{-}2\text{-}SC_5H_4N)Cl(PPh_3)_2]$ (**10**), $[ReO(\eta^2\text{-}2\text{-}SC_4H_3N_2)_2(\eta^1\text{-}2\text{-}SC_4H_3N_2)]$ (**11**), and $[Re(PPh_3)(\eta^2\text{-}2\text{-}SC_4H_3N_2)_3]$ (**12**), were characterized by analytical and spectroscopic methods and, in the cases of **5**−**7** and **9**−**12**, by X-ray crystallography. Furthermore, convenient preparations of **5** and **6**, two potentially useful rhenium(V) starting materials, are presented.

Experimental Section

General Considerations. NMR spectra were recorded on a General Electric QE 300 (^{1}H 300.10 MHz) spectrometer in $CDCl_3$ (δ 7.24), CD_2Cl_2 (δ 5.32), or CD_3CN (δ 1.93). Variable-temperature ^{1}H NMR spectra utilized a Doric Trendicator 410A temperature controller. IR spectra were recorded as KBr pellets with a Perkin-Elmer Series 1600 FTIR, and UV−visible spectra were recorded as solutions in quartz cuvettes on a Cary 1E spectrophotometer. Electrochemical experiments were performed by using a BAS CV-27 cyclic voltammograph and a BAS Model RXY recorder. A three-compartment, gas-adapted cell was used with a glassy carbon working electrode, a platinum wire auxiliary electrode, and a silver/silver chloride reference electrode. Cyclic voltammograms were recorded under N_2 in dry, distilled CH_2Cl_2 which was 0.1 M in supporting electrolyte (tetrabutylammonium hexafluorophosphate [TBAP]) and 2 mM in sample. The potentials are reported versus silver/silver chloride and ferrocene. Elemental analyses for carbon, hydrogen, and nitrogen were carried out by Oneida Research Services, Whitesboro, NY.

All synthetic manipulations, except for those noted, were carried out by utilizing standard Schlenk techniques under dry N_2, and solvents

(12) Meares, C. F. In *Protein Tailoring for Food and Medical Uses*; Feeney, R. F., Whiteker, J. R., Eds.; Marcel Dekker, New York, 1986; p 339. Yeh, S. M.; Sherman, D. G.; Meares, C. F. *Anal. Chem.* **1979**, *100*, 152. Meares, C. F.; Wensel, T. G. *Acc. Chem. Res.* **1984**, *17*, 202. Brechbiel, M. W.; Gansow, O. A.; Atcher, R. W.; Schlom, J.; Esteban, J.; Simpson, D. E.; Colcher, D. *Inorg. Chem.* **1986**, *25*, 2772 and references therein.

(13) For the specific case of ^{99m}Tc labeling see: Lanteigne, D. D.; Hnatowich, D. J. *Int. J. Appl. Radiat. Isot.* **1984**, *35*, 617. Arano, Y.; Yokoyama, A.; Furukawa, T.; Horiuchi, K.; Yahata, T.; Saji, H.; Sakahara, H.; Nakashima, T.; Koizumi, M.; Endo, K.; Torizuka, K. *J. Nucl. Chem.* **1987**, *28*, 1027. Fritzberg, A. Eur. Patent Appl. EP 188256 2A. Liang, F. H.; Virzi, F.; Hnatowich, D. J. *Nucl. Med. Biol.* **1987**, *14*, 63. Lever, S. Z.; Baidoo, K. E.; Kramer, A. V.; Burns, H. D. *Tetrahedron Lett.* **1988**, *29*, 3219. Eary, J. F.; Schroff, R. F.; Abrams, P. G.; Fritzberg, A. R.; Morgan, A. C.; Kasina, S.; Reno, J. M.; Srinivasan, A.; Woodhouse, C. S.; Wilbur, D. S.; Natale, R. B.; Collins, C.; Stehlin, J. S.; Mitchell, M.; Nelp, W. B. *J. Nucl. Med.* **1989**, *30*, 25.

(14) Abrams, M. J.; Shaikh, S. N.; Zubieta, J. *Inorg. Chim. Acta* **1990**, *173*, 133.

(15) Abrams, M. J.; Larsen, S. K.; Zubieta, *J. Inorg. Chim. Acta* **1990**, *171*, 133.

(16) Abrams, M. J.; Chen, Q.; Shaikh, S. N.; Zubieta, J. *Inorg. Chim. Acta* **1990**, *176*, 11.

(17) Abrams, M. J.; Larsen, S. K.; Zubieta, J. *Inorg. Chem.* **1991**, *30*, 2031.

(18) Abrams, M. J.; Larsen, S. K.; Shaikh, S. N.; Zubieta, J. *Inorg. Chim. Acta* **1991**, *185*, 7.

(19) Schwartz, D. A.; Abrams, M. J.; Hauser, M. M.; Gaul, F. E.; Larsen, S. K.; Rauh, D.; Zubieta, J. *Bioconjugate Chem.* **1991**, *2*, 333.

(20) Abrams, M. J.; Juweid, M.; ten Kate, C. I.; Schwartz, D. A.; Hauser, M. M.; Gaul, F. E.; Fuccello, A. J.; Rubin, R. H.; Strauss, H. W.; Fischman, A. J. *J. Nucl. Med.* **1990**, *31*, 2022.

(21) Nicholson, T.; Zubieta, J. *Polyhedron* **1988**, *7*, 171.

(22) Nicholson, T.; Zubieta, J. *Inorg. Chem.* **1987**, *26*, 2094 and references therein.

(23) Nicholson, T.; Zubieta, J. *Inorg. Chim. Acta* **1987**, *134*, 191.

(24) Nicholson, T.; Lombardi, P.; Zubieta, J. *Polyhedron* **1987**, *6*, 1577.

(25) Nicholson, T.; Shaikh, S. N.; Zubieta, J. *Inorg. Chem.* **1988**, *27*, 241.

(26) Nicholson, T.; Shaikh, S. N.; Zubieta, J. *Inorg. Chim. Acta* **1985**, *99*, L45.

(27) Nicholson, T.; Zubieta, J. *J. Chem. Soc., Chem. Commun.* **1985**, 367.

(28) Kettler, P. B.; Chang, Y.-D.; Zubieta, J.; Abrams, M. J. *Inorg. Chem.*, in press.

(29) Reynolds, J. G.; Sendlinger, S. C.; Murray, A. M.; Huffman, J. C.; Christou, G. *Angew. Chem., Int. Ed. Engl.* **1992**, *31*, 1253.

(30) Zhang, N.; Wilson, S. R.; Shapley, P. A. *Organometallics* **1988**, *7*, 1128.

(31) Gilbert, J. D.; Rose, D.; Wilkinson, G. *J. Chem. Soc. A* **1970**, 2765.

(32) Kitagawa, S.; Munakata, M.; Shimono, H.; Matsuyama, S.; Masuda, H. *J. Chem. Soc., Dalton Trans.* **1990**, 2105.

(33) Cotton, F. A.; Fanwick, P. E.; Fitch, J. W., III. *Inorg. Chem.* **1978**, *17*, 3254.

(34) Constable, E. C.; Raithby, P. R. *J. Chem. Soc., Dalton Trans.* **1987**, 2281.

(35) Block, E.; Gernon, M.; Kang, H.; Zubieta, J. *Angew. Chem., Int. Ed. Engl.* **1988**, *27*, 1342.

(36) Block, E.; Brito, M.; Gernon, M.; McGowty, D.; Kang, H.; Zubieta, J. *Inorg. Chem.* **1990**, *29*, 3173.

(37) Block, E.; Gernon, M.; Kang, H.; Liu, S.; Zubieta, J. *Inorg. Chim. Acta* **1990**, *167*, 143.

(38) Block, E.; Macherone, D.; Shaikh, S. N.; Zubieta, J. *Polyhedron* **1990**, *9*, 1429.

(39) Block, E.; Gernon, M.; Kang, H.; Ofori-Okai, G.; Zubieta, J. *Inorg. Chem.* **1991**, *30*, 1736.

(40) Castro, R.; García-Vázquez, J. A.; Romero, J.; Sousa, A.; Castñeiras, A.; Hiller, W.; Strähle, J. *Inorg. Chim. Acta* **1993**, *211*, 47.

(41) Deeming, A. J.; Karim, M.; Bates, P. A.; Hursthouse, M. B. *Polyhedron* **1988**, *7*, 1401.

(42) Deeming, A. J.; Karim, M.; Powell, N. I.; Hardcastle, K. I. *Polyhedron* **1990**, *9*, 623.

(43) Cockerton, B.; Deeming, A. J.; Karim, M.; Hardcastle, K. I. *J. Chem. Soc., Dalton Trans.* **1991**, 431.

were distilled from their appropriate drying agents.[44] Triethylamine (Aldrich) was distilled from CaH_2 and stored under an inert atmosphere. Pyridine-2-thiol (Aldrich), pyrimidine-2-thiol (Aldrich), chlorotrimethylsilane (Petrarch), *tert*-butyldimethylchlorosilane (Petrarch), *n*-butyllithium (2.5 M solution in hexanes; Aldrich), benzoylhydrazine (Aldrich), triphenylphosphine (Aldrich), bromine (Aldrich), cyclohexene (Fisher), toluene (Sure-Seal; Aldrich), and other reagents were used as received without further purification. Tetrabutylammonium perrhenate was prepared by mixing aqueous solutions of tetrabutylammonium bromide and ammonium perrhenate, collecting the precipitated colorless solid via vacuum filtration on a frit, and recrystallization of the product from THF/H_2O. The reagents **2**,[39] **3**,[39] $[ReOCl_3(PPh_3)_2]$,[45] $[Re(N_2CO(C_6H_5)Cl_2(PPh_3)_2]$,[46] and tetrabutylammonium hexafluorophosphate were synthesized by published procedures.[47]

Syntheses. Preparation of Pyridine-2-thiol (1). The yellow crystalline solid was prepared by the method of Katritzky.[48] The crude product was rotovapped to dryness and Soxhlet-extracted with benzene until no color was evident in the extract. The extract was rotovapped to dryness, the solid dissolved in acetone, and the mixture filtered. The acetone was removed by rotary evaporation, and the resulting solid was stirred with 125 mL of pentane overnight. The mixture was filtered, and the solid was dried under vacuum to give pyridine-2-thiol in 31% yield. IR (KBr pellet, cm^{-1}): 2958 (m), 2876 (m), 1734(w), 1654(w), 1571 (vs), 1491 (m), 1438 (m), 1366 (s), 1257 (m), 1180 (m), 1137 (vs), 982 (m), 742 (s), 486 (s).

Preparation of 3-(Trimethylsilyl)pyridine-2-thiol (2). The yellow crystalline solid was prepared by the method of Block.[49] After sublimation, the crude product (102.4% yield) was washed with acetone and pentane, and crystals were grown by diffusion of pentane into a CH_2Cl_2 solution of the ligand. Recrystallized yield: 40%. IR (KBr pellet, cm^{-1}): 2940 (s), 2854 (s), 1604 (s), 1572 (s), 1309 (vs), 1236 (s), 1203 (m), 1150 (vs), 1122 (s), 1064 (m), 1041 (s), 851 (vs), 749 (vs), 622 (m), 512 (w), 475 (m).

Preparation of 3,6-Bis(*tert*-butyldimethylsilyl)pyridine-2-thiol (3). The yellow crystalline solid was prepared by the method of Block.[50] The crude product was quenched with H_2O and neutralized with HCl. The mixture was rotary-evaporated to dryness, dissolved in CH_2Cl_2, and then extracted with water. The aqueous layers were extracted with CH_2Cl_2, and the CH_2Cl_2 extracts were combined and dried over $MgSO_4$. The solution was filtered, and the filtrate was rotary-evaporated to dryness. The desired product was then sublimed from the crude reaction mixture. The sublimed product was further purified by washing with hexanes, to give 6.4 g of pure product (63% yield). IR (KBr pellet, cm^{-1}): 2940 (w), 2849 (w), 1565 (m), 1468 (m), 1289 (s), 1259 (s), 1160 (m), 1141 (s), 1098 (s), 1033 (m), 804 (s), 677 (m), 581 (w), 500 (w).

Preparation of $[Bu_4N][ReOBr_4(H_2O)]\cdot 2H_2O$ (5). All steps were performed open to the atmosphere. To a solution of PBu^n_3 (2.842 g, 14.05 mmol) in 20 mL of CH_2Cl_2 was added a solution of Br_2 (2.269 g, 14.20 mmol) in 20 mL of CH_2Cl_2 dropwise via pipet. The generated purple phosphorane solution ($Bu^n_3PBr_2$) was then added to a colorless solution of $[Bu_4N][ReO_4]$ (2.000 g, 4.06 mmol) in 20 mL of CH_2Cl_2 in the presence of O_2 (open air). The red-violet reaction mixture was stirred 45 min after complete addition of the phosphorane. After 45 min, 100 mL of ether, 3 mL of cyclohexene, and 100 mL of pentane were added to the reaction mixture and a violet solid precipitated from the reaction mixture. The product was collected via vacuum filtration on a frit, washed with ether, and air-dried (3.0 g, 3.1 mmol, 75%). Anal. Calcd for $C_{28}H_{65}NO_2PReBr_4$ (mol wt 983.77): C, 34.15; H, 6.60; N, 1.42. Found: C, 34.53; H, 6.46; N, 1.51. IR (KBr, cm^{-1}): 2961 (s), 2872 (m), 1466 (s), 1381 (w), 1226 (w), 993 (vs), 808 (w), 738 (w). X-ray quality crystals of **5** were prepared by diffusion of Et_2O into a solution of $C_{28}H_{65}NO_2PReBr_4$ in CH_2Cl_2. During the crystallization, one tributylphosphine was lost and replaced with two water molecules.

Preparation of $[Bu_4N][ReOBr_4(OPPh_3)]$ (6). All steps were performed open to the atmosphere. To a solution of PPh_3 (1.06 g, 4.05 mmol) in 10 mL of CH_2Cl_2 was added a solution of Br_2 (0.205 mL, 4.05 mmol) in 10 mL of CH_2Cl_2 dropwise via pipet. A water bath was used to cool the solution during addition. The generated purple phosphorane solution (Ph_3PBr_2) was then stirred for 2 h before being added to a colorless solution of $[Bu_4N][ReO_4]$ (0.500 g, 4.05 mmol) in 10 mL of CH_2Cl_2 in the presence of O_2 (open air). To the red-violet reaction mixture was added 100 mL of ether, 100 mL of pentane, and 0.75 mL of cyclohexene, and a violet solid precipitated from the reaction mixture. The product was collected via filtration and air-dried (2.12 g, 2.03 mmol, 51%). Anal. Calcd for $C_{52}H_{66}NO_2P_2ReBr_4$ (mol wt 1303.74): C, 47.86; H, 5.06; N, 1.07. Found: C, 47.61; H, 5.56; N, 1.37. IR (KBr, cm^{-1}): 2961 (m), 2872 (m), 1458 (s), 1438 (s), 1146 (s), 1120 (s), 1090 (m), 994 (vs), 932 (m), 878 (m), 724 (m), 693 (m), 537 (s). X-ray quality crystals of **6** were prepared by diffusion of Et_2O into a solution of $C_{52}H_{66}NO_2P_2ReBr_4$ in CH_2Cl_2. During the crystallization one triphenylphosphine was lost.

Preparation of $[ReO_2(C_5H_5N)_4]Cl\cdot 2H_2O$.[51] All steps were performed open to the atmosphere. To a solution of 5 g (19 mmol) of PPh_3 in 30 mL of EtOH was added a solution of 3.5 mL (30 mmol) of 37% HCl containing 1 g (3.73 mmol) of NH_4ReO_4. The solution was refluxed in a 50 mL Schlenk flask for 10 min. The color of the solution changed from milky white to olive. The reaction mixture was cooled to room temperature and filtered. The precipitate was washed with two 10 mL portions of EtOH and two 10 mL portions of Et_2O to yield $[ReOCl_2(OEt)(PPh_3)_2]$ in quantitative yield (3 g).

To a gray-green solution of $[ReOCl_2(OEt)(PPh_3)_2]$ (1 g, 1.19 mmol) in 25 mL of EtOH was added dropwise 5 mL (62 mmol) of pyridine. The solution was refluxed for 2 h, whereupon the volume was reduced under vacuum to 10 mL. The product was recrystallized from EtOH/Et_2O, collected by filtration, and dried in the air to give $[ReO_2(C_5H_5N)_4]Cl\cdot 2H_2O$ (0.7 g, 95% yield). IR (KBr, cm^{-1}): 3382 (s), 3063 (m), 1604 (m), 1477 (m), 1447 (s), 1345 (m), 1209 (m), 1150 (w), 1068 (m), 820 (s), 778 (s), 704 (s), 468 (w).

Preparation of $[ReO(\eta^2\text{-}2\text{-}SC_5H_4N)_2(\eta^1\text{-}2\text{-}SC_5H_4N)]$ (7). To a solution of **5** (0.250 g, 0.25 mmol) in 15 mL of THF at 0 °C was added a solution of **1** (0.107 g, 0.96 mmol) and Et_3N (0.097 g, 0.96 mmol) in 5 mL of THF dropwise via syringe. Upon addition, the reaction mixture changed in color from violet to dark green, with a colorless solid (Et_3NHBr) precipitating from the reaction mixture. After being stirred for 2 h, the reaction mixture was filtered to remove the precipitated triethylamine hydrobromide and the filtrate evaporated to dryness. Recrystallization of the crude product from CH_2Cl_2/ether afforded dark green blocks of **7** (0.070 g, 0.13 mmol, 55%). Anal. Calcd for $C_{15}H_{12}N_3OReS_3$ (mol wt 532.70): C, 33.82; H, 2.27; N, 7.89. Found: C, 34.40; H, 2.44; N, 8.94. IR (KBr, cm^{-1}): 3044 (w), 1584 (vs), 1568 (sh), 1554 (m), 1439 (s), 1414 (s), 1264 (s), 1142 (w), 1120 (w) 1039 (w), 962 (m), 954 (sh), 803 (w), 761 (vs), 736 (w), 647 (w), 484 (w). ^1H NMR ($CDCl_3$, 293 K): all resonances are coalesced into the baseline. UV−vis (λ_{max}, nm (ϵ, $M^{-1}\ cm^{-1}$) in CH_2Cl_2): 242 (1.06×10^4), 285 (1.04×10^4), 365 (6.3×10^3), 650 (90).

Preparation of $[ReO(\eta^2\text{-}2\text{-}SC_5H_3N\text{-}3\text{-}SiMe_3)_2(\eta^1\text{-}2\text{-}SC_5H_3N\text{-}3\text{-}SiMe_3)]$ (8). Compound **5** (0.250 g, 0.25 mmol), **2** (0.176 g, 0.96 mmol), and Et_3N (0.096 g, 0.96 mmol) were mixed in 20 mL of THF as described for **7**. Recrystallization of the crude product from a concentrated solution of hexanes at −20 °C afforded **8** as a green microcrystalline solid (0.059 g, 0.079 mmol, 33%). Anal. Calcd for $C_{24}H_{36}N_3OReS_3Si_3$ (mol. wt. 749.24): C, 38.47; H, 4.84; N, 5.61. Found: C, 38.38; H, 4.10; N, 5.74. IR (KBr, cm^{-1}): 2959 (m), 1560 (m), 1539 (w), 1368 (vs), 1249 (m), 1080 (w), 1022 (w), 966 (m), 841 (vs), 801 (w), 760 (w). ^1H NMR (CD_2Cl_2, 243 K): δ 8.68 (bd, 1H), 8.56 (bd, 1H), 7.80 (m, 2H), 7.65 (d, 1H), 7.26 (dd, $J = 6.8$ Hz, 1.3 Hz, 1H), 7.07 (m, 2H), 6.37 (t, $J = 6.3$ Hz, 1H), 0.44 (s, 9H), 0.33 (s, 9H), 0.20 (s, 9H).

Preparation of $[ReO(OH)(\eta^2\text{-}SC_5H_2N\text{-}3,6\text{-}(SiMe_2Bu^t)_2)_2]$ (9). Compound **5** (0.250 g, 0.25 mmol), **3** (0.326 g, 0.96 mmol), and Et_3N (0.097

(44) Perrin, D. D.; Armarego, W. L. F.; Perrin, D. R. *Purification of Laboratory Chemicals*; Pergamon Press: London, 1980.
(45) Parshall, G. W. *Inorg. Synth.* **1977**, *17*, 100.
(46) Chatt, J.; Dilworth, J. R.; Leigh, G. J.; Gupta, V. D. *J. Chem. Soc. A* **1971**, 2631.
(47) Ferguson, J. A. *Interface* **1970**, *6* (2), 1.
(48) Jones, R. A.; Katritzky, A. R. *J. Chem. Soc.* **1958**, 3610.
(49) Block, E.; Gernon, M.; Kang, H.; Zubieta, J. *Angew. Chem., Int. Ed. Engl.* **1988**, *27*, 1342−1344.
(50) Block, E.; Gernon, M.; Kang, H.; Ofari-Okai, G.; Zubieta, J. *Inorg. Chem.* **1991**, *30*, 1736.
(51) Chang, L.; Rall, J.; Tisato, F.; Deutsch, E.; Heeg, M. J. *Inorg. Chim. Acta* **1993**, *205*, 35−41.

Table 1. Crystallographic Data for the Structural Studies of $[ReOBr_4(H_2O)]\cdot 2H_2O$ (**5**), $[ReOBr_4(OPPh_3)]$ (**6**), $[ReO(SC_5H_4N)_3]$ (**7**), $[ReO(OH)(SC_5H_2N\text{-}3,6\text{-}(SiMe_2Bu^t)_2)_2]$ (**9**), $[Re(N_2CO(C_6H_5))(SC_5H_4N)Cl(PPh_3)_2]$ (**10**), $[ReO(SC_4H_2N_2)_3]$ (**11**), and $[Re(PPh_3)(SC_4H_2N_2)_3]$ (**12**)

	5	**6**	**7**	**9**	**10**	**11**	**12**
empirical formula	$C_{16}H_{42}NO_4Br_4Re$	$C_{34}H_{51}O_2PBr_4Re$	$C_{15}H_{12}N_3OS_3Re$	$C_{34}H_{65}N_2O_2S_2Si_4Re$	$C_{48}H_{39}N_3OSP_2ClRe$	$C_{12}H_9N_6OS_3Re$	$C_{31}H_{26}N_6S_3PClRe$
a, Å	12.228(2)	14.437(2)	11.533(2)	8.072(2)	10.842(2)	8.240(2)	9.224(2)
b, Å	12.290(2)	16.589(3)	11.385(2)	11.409(2)	13.660(3)	13.373(3)	12.050(2)
c, Å	20.014(2)	16.783(3)	14.039(3)	12.402(2)	17.665(4)	29.388(6)	17.665(4)
α, deg		94.87(2)		79.67(3)	86.37(3)		89.25(3)
β, deg		97.62(2)	107.97(3)	74.05(3)	89.93(3)		85.70(3)
γ, deg		93.80(2)		86.18(3)	77.22(3)		67.94(3)
V, Å^3	3022.61(4)	3957(1)	1749.8(9)	1080.2(5)	2080.2(10)	3238.4(2)	1604.0(8)
Z	4	4	4	1	2	8	2
fw	818.3	661.8	760.4	896.6	670.2	2254.2	866.9
space group	$I\bar{4}$	$P\bar{1}$	$P2_1/c$	$P\bar{1}$	$P\bar{1}$	Pbca	$P\bar{1}$
T, °C	−60	−60	−60	−60	−60	−60	−40
λ, Å	0.710 73	0.710 73	0.710 73	0.710 73	0.710 73	0.710 73	0.710 73
D_{calc}, g cm^{-3}	1.798	1.749	1.218	1.378	1.579	2.197	1.795
μ, cm^{-1}	96.17	71.78	73.10	30.05	63.98	79.03	42.33
R^a	0.0457	0.0758	0.0322	0.0525	0.0437	0.0512	0.0697
$R_w{}^b$	0.0606	0.0902	0.0434	0.0776	0.0591	0.0562	0.0848

^{a} $\sum||F_o| - |F_c||/\sum|F_o|$. ^{b} $[\sum w(|F_o| - |F_c|)^2/\sum w|F_o|^2]^{1/2}$.

g, 0.96 mmol) were reacted as described for **7**. Upon dissolution of the light green crude product for purification in CH_2Cl_2, the solution turned orange-brown. Recrystallization of the crude product from CH_2Cl_2/CH_3OH afforded **9** as tan-brown needles (0.056 g, 0.062 mmol, 26%). The formulation of this complex was confirmed by X-ray crystallography. IR (KBr, cm^{-1}): 3439 (m), 2942 (m), 2854 (w), 1466 (w), 1388 (m), 1289(w), 1256 (m), 1095 (s), 1025 (m), 952 (m), 806 (vs). ^{1}H NMR ($CDCl_3$, 293K): δ 7.73 (d, J = 7.8 Hz, 2H), 7.4 (b, 2H) 1.00 (s, 18H), 0.97 (s, 18H), 0.49 (s, 9H), 0.43 (s, 9H). UV−vis (λ_{max}, nm (ϵ, M^{-1} cm^{-1}) in CH_2Cl_2): 245 (9.3 × 10^3), 306 (9.8 × 10^3), 370 (9.6 × 10^3), 400 (8.1 × 10^3), 680 (2.2 × 10^2).

Preparation of [Re{η^1-N$_2$CO(C$_6$H$_5$)}(η^2-2-SC$_5$H$_4$N)Cl(PPh$_3$)$_2$] (10). To a solution of $[Re\{N_2CO(C_6H_5)\}Cl_2(PPh_3)_2]$ (0.250 g, 0.27 mmol) in 40 mL of toluene was added a solution of **1** (0.091 g, 0.82 mmol) and Et_3N (0.083 g, 0.82 mmol) in 10 mL of toluene dropwise via syringe. The dark green reaction mixture was heated to 50 °C and stirred for 12 h. After this time, the reaction mixture was cooled to −20 °C and filtered to remove the insoluble precipitate (Et_3NHCl). Upon reduction of the filtrate to 5 mL and layering of hexanes onto the concentrated solution, an emerald green microcrystalline solid crystallized from solution (0.135 g, 50% yield). X-ray quality crystals were grown by diffusing hexanes into a toluene solution of **10** for a second time. Anal. Calcd for $C_{48.25}H_{39.5}Cl_{1.5}N_3OP_2ReS$ (**10**·0.25CH_2Cl_2): C, 57.30; H, 3.93; N, 4.15. Found: C, 57.68; H, 3.96; N, 4.33. IR (KBr, cm^{-1}): 3056 (w), 2456 (w), 1653 (m), 1557 (m), 1498 (m), 1471 (m), 1437 (m), 1260 (m), 1227 (vs), 1166 (w), 1089 (m), 1033 (w), 1011 (w), 801 (m), 745 (m), 696 (m), 635 (w), 513 (m). ^{1}H NMR (CD_3CN, 293 K): δ 8.79 (s, 1H), 8.04 (d, 2H), 7.71 (b, 12H), 7.46 (t, J = 7.1 Hz, 1H), 7.32 (t, J = 7.7 Hz, 2H), 7.23 (m, 18H), 6.60 (t, J = 6.6 Hz, 1H), 6.00 (d, J = 8.1 Hz, 1H), 5.59 (t, J = 6.4 Hz, 1H). $E_{1/2}$ (cyclic voltammetry, CH_2Cl_2): +0.27 V (ΔE_p = 60 mV). UV−vis (λ_{max}, nm (ϵ, M^{-1} cm^{-1}) in CH_2Cl_2): 233 (6.86 × 10^3), 277 (6.65 × 10^3), 367 (3.91 × 10^3).

Preparation of [ReO(C$_4$H$_3$N$_2$S)$_3$] (11). All steps were performed open to the atmosphere. $[ReO_2(C_5H_5N)_4]Cl\cdot 2H_2O$ (0.2 g, 0.33 mmol), pyrimidine-2-thiol (0.11 g, 0.99 mmol), and 10 mL of EtOH were placed in a 50 mL Schlenk flask. After addition of NEt_3 (0.13 mL, 0.99 mmol), the mixture was refluxed for 3 h. The reaction mixture was filtered to produce a green precipitate of $[ReO(C_5H_3N_2S)_3]$ in 61% yield. Anal. Calcd for $C_{12}H_9N_6OReS_3$: C, 26.90; H, 1.68; N, 15.69. Found: C, 27.92; H, 1.77; N, 15.39. IR (KBr, cm^{-1}): 3448 (w), 3060 (w), 2943 (w), 2674 (w), 2496 (w), 2377 (w), 1561 (s), 1544 (s), 1429 (m), 1372 (vs), 1261 (w), 1193 (m), 1169 (m), 967 (s), 805 (m), 762 (m). ^{1}H NMR: 7.18−7.34 ppm. X-ray quality crystals were grown by diffusion of pentane into a CH_2Cl_2 solution of **11**, $[ReO(C_4H_3N_2S)_3]$. The filtrate was vacuumed down to yield a brown residue of **12**, $[Re\{P(C_6H_5)_3\}(C_4H_3N_2S)_3]$, as a minor product of the reaction.

Preparation of [Re(PPh$_3$)(C$_4$H$_3$N$_2$S)$_3$] (12). All steps were performed open to the atmosphere. To a solution of PPh_3 (5.00 g, 19 mmol) in 30 mL of EtOH was added a solution of 37% HCl (3.5 mL, 30 mmol) containing NH_4ReO_4 (1.00 g, 3.73 mmol). The solution was refluxed in a 50 mL Schlenk flask for 10 min, whereupon its color changed from milky white to olive. The reaction mixture was cooled to room temperature and filtered. The precipitate was washed with two 10 mL portions of EtOH and two 10 mL portions of Et_2O to yield $[ReOCl_2(OEt)(PPh_3)_2]$ in a quantitative yield (3 g).

To gray-green $[ReOCl_2(OEt)(PPh_3)_2]$ (0.100 g, 0.119 mmol) were added pyrimidine-2-thiol (0.039 g, 0.356 mmol) and 10 mL of EtOH, followed by NEt_3 (0.049 mL, 0.356 mmol). The solution was refluxed for 12 h. The product was recrystallized from EtOH/Et_2O to give **12** in quantitative yield. IR (KBr, cm^{-1}): 3433 (m), 2964 (m), 2676 (m), 2366 (m), 1607 (m), 1377 (m), 1331 (m), 1187 (m), 1036 (w), 911 (s), 796 (m). ^{1}H NMR: 7.1−7.9, 8.5−8.6 ppm. X-ray quality crystals were grown by diffusion of pentane into a CH_2Cl_2 solution of **12**.

X-ray Crystallography. Compounds **5**−**7** and **9**−**12** were studied using a Rigaku AFC5S diffractometer, equipped with a low-temperature device. Since the crystals of **7** and **9**−**12** degraded slowly at room temperature, data collections were carried out at low temperature. Crystal stability was monitored using five medium-intensity reflections in each case, and no significant changes in the intensities of the standards were observed over the course of the data collections. The crystal parameters and other experimental details of the data collections are summarized in Table 1. A complete description of the details of the crystallographic methods is given in the Supporting Information.

The structures were solved by the Patterson method and refined by full-matrix least squares. The details of the structure solutions and refinements are presented in the Supporting Information. No anomalies were encountered in the refinements of the structures of **5**−**7** and **10**−**12**. In the case of **9**, the {Re═O} unit was disordered along the {ReO(OH)} vector. The disorder was modeled by assigning populations of 0.70 and 0.30 for the two sites, respectively. Although the excursions of electron density of *ca.* 1 e/Å^3 were found along this axis on the final difference map, the model was deemed adequate in other respects.

Attempts to refine the structure of **9** in the centric space group $P\bar{1}$ resulted in unreasonable temperature factors and unacceptable geometry for the carbon framework of the ligand.

Atomic positional parameters and isotropic temperature factors for the structures are presented in Tables 2−8, and selected bond lengths and angles are given in Tables 9−15.

Results and Discussion

Preparation of [Bu$_4$N][ReOBr$_4$(H$_2$O)]·2H$_2$O and [Bu$_4$N][ReOBr$_4$(OPPh$_3$)]. In many diagnostic radiopharmaceutical preparations employing ^{99m}Tc, the complex $TcOCl_4^-$, prepared directly from the $^{99m}TcO_4^-$ solution eluted from the generator column, is utilized as a precursor in clinical applications. In developing an analogous system with ^{186,188}Re, it was found that the $ReOCl_4^-$ anion is too moisture sensitive for this application. Therefore, it was necessary to adopt as a convenient

Table 2. Atomic Positional Parameters ($\times 10^4$) and Isotropic Temperature Factors ($Å^2 \times 10^3$) for the Anion $[ReOBr_4(H_2O)]^- \cdot 2H_2O$ in **5**

	x	*y*	*z*	*U*(eq)[a]
Re(1)	5000	0	430(1)	38(2)
Br(2)	3552(8)	1403(8)	594(6)	68(4)
Br(2)	6455(7)	1415(8)	598(5)	52(4)
O(1)	5000	0	−365(15)	68(9)
O(2)	5000	0	1568(12)	46(7)
N(1)	5000	5000	0	19(25)
C(1)	4127(36)	4588(35)	451(18)	58(12)
C(2)	3697(41)	4740(45)	935(21)	69(14)
C(3)	2345(42)	4495(45)	1363(21)	59(33)
C(4)	1670(43)	5477(46)	1655(22)	71(37)
N(2)	10000	0	0	82(51)
C(5)	442(36)	1026(34)	464(17)	72(15)
C(6)	432(37)	1601(36)	924(20)	112(23)
C(7)	10106(45)	2299(41)	1290(24)	71(14)
C(8)	43(46)	3103(42)	1670(24)	32(30)
O(3)	2449(35)	486(42)	2500(24)	89(16)
O(4)	7101(34)	1324(69)	2491(25)	125(29)

[a] Equivalent isotropic *U* defined as one-third of the trace of the orthogonalized $\mathbf{U}_{ij}$ tensor.

starting material the $ReOBr_4^-$ anion,[52] which also serves as an ideal precursor in this study of rhenium model complexes for the bifunctional chelate technology described in the Introduction. However, under our conditions, the literature method for the preparation of $ReOBr_4^-$ with a variety of large cations (i.e. Bu_4N^+, Ph_4^+) could not be reproduced. Instead, the reaction in open air of $[Bu_4N][ReO_4]$ with excess $Bu^n{}_3PBr_2$ (prepared *in situ* from $PBu^n{}_3$ and Br_2) yields the $[ReOBr_4(H_2O)]^-$ anion as shown in eq 1. The use of PPh_3 in place of PBu_3 results in

$$3Br_2 + 3PBu^n{}_3 \xrightarrow{CH_2Cl_2} 3Bu^n{}_3PBr_2$$

$$3Bu^n{}_3PBr_2 + [Bu_4N]^+[ReO_4]^- \xrightarrow[\text{cyclohexene}]{CH_2Cl_2} [Bu_4N]^+[ReOBr_4(H_2O)]^- \cdot PBu^n{}_3 \quad (1)$$

5

the isolation of the triphenylphosphine oxide adduct of the $ReOBr_4^-$ anion. Furthermore, it is necessary to perform the reaction in the open air since, under inert conditions, an orange crystalline solid, presumably $[Bu_4N]_2[ReBr_6]$, is formed rather than $[ReOBr_4(H_2O)]^-$ **(5)**.

The IR spectrum for **5** displays ν(C−H) for the $[Bu_4N]^+$ cation at 2961 and 2872, ν(C−C) at 1466 cm^{-1}, and a feature assigned to ν(Re═O) at 993 cm^{-1}. This violet complex, **5**, is indefinitely air and moisture stable and was used to probe the reactivity of **1**−**3** with high-valent rhenium.

Synthesis and Spectroscopic Characterization of High-Valent Rhenium Pyridinethiolate Complexes. The synthesis of $[ReO(\eta^2\text{-}2\text{-}SC_5H_4N)_2(\eta^1\text{-}2\text{-}SC_5H_4N)]$ (**7**) and $[ReO(\eta^2\text{-}2\text{-}SC_5H_3N\text{-}3\text{-}SiMe_3)_2(\eta^1\text{-}2\text{-}SC_5H_3N\text{-}3\text{-}SiMe_3)]$ (**8**) proceeds by the reaction of either **5** or $[ReOCl_3(PPh_3)_2]$ with excess pyridine-2-thiol **(1)** or 3-(trimethylsilyl)pyridine-2-thiol **(2)** in the presence of Et_3N in THF at 0 °C, as shown in eq 2. A solution of the pyridine-2-thiol ligand and triethylamine in THF was transferred via syringe to a violet solution of 3,6-bis(dimethyl-*tert*-butylsilyl)pyridine-2-thiol **(3)** in THF at 0 °C. Upon addition of the pyridine-2-thiolate solution, the reaction mixture turned from violet to dark green, with a colorless solid (Et_3-NHBr) precipitating out of solution. The crude product was recrystallized from CH_2Cl_2/ether, giving a dark green crystalline solid in moderate yield. Elemental analysis for **7** indicates that

(52) Cotton, F. A.; Lippard, S. J. *Inorg. Chem.* **1966**, *5*, 9.

Table 3. Atomic Positional Parameters ($\times 10^4$) and Isotropic Temperature Factors ($Å^2 \times 10^3$) for the Anion $[ReOBr_4(OPPh_3)]^-$ in **6**

	x	*y*	*z*	*U*(eq)[a]
Re(1)	3384(1)	2137(1)	4825(1)	38(1)
Re(2)	3595(1)	6986(1)	−234(1)	36(1)
Br(1)	3944(2)	2745(2)	6247(2)	61(1)
Br(2)	3282(2)	750(2)	5333(2)	57(1)
Br(3)	2532(2)	1449(2)	3476(2)	70(1)
Br(4)	3123(2)	3532(2)	4388(2)	68(1)
Br(5)	2969(2)	6644(2)	−1723(2)	52(1)
Br(6)	3896(2)	7425(2)	1259(2)	52(1)
Br(7)	2788(2)	5687(2)	97(2)	50(1)
Br(8)	4116(2)	8414(2)	−500(2)	59(1)
O(1)	2034(10)	2221(9)	5145(9)	38(6)
O(2)	4355(12)	2084(10)	4607(11)	68(8)
O(3)	2292(11)	7442(9)	−162(9)	44(6)
O(4)	4552(11)	6638(10)	−328(9)	50(7)
P(1)	1137(4)	2510(4)	5410(4)	32(2)
P(2)	1241(4)	7539(4)	−244(3)	34(2)
N(1)	4255(14)	4710(11)	2400(10)	40(7)
N(2)	4872(15)	9902(11)	2467(11)	47(8)
C(1)	1332(14)	3179(13)	6323(13)	27(5)
C(2)	1920(16)	3893(15)	6327(15)	45(7)
C(3)	2044(17)	4464(16)	7069(16)	50(7)
C(4)	1663(18)	4296(17)	7700(17)	58(8)
C(5)	1120(18)	3571(17)	7697(17)	57(8)
C(6)	931(17)	3035(16)	6985(15)	51(7)
C(7)	380(15)	1656(13)	5583(13)	30(5)
C(8)	−537(19)	1636(18)	5476(17)	63(8)
C(9)	−1119(19)	952(17)	5595(16)	59(8)
C(10)	−707(20)	327(19)	5851(17)	66(9)
C(11)	287(18)	306(18)	6015(17)	64(8)
C(12)	813(17)	986(15)	5854(15)	48(7)
C(13)	500(15)	3059(14)	4654(14)	36(6)
C(14)	−13(18)	3686(17)	4869(17)	60(8)
C(15)	−547(17)	4030(16)	4300(16)	53(7)
C(16)	−604(21)	3805(19)	3490(19)	74(9)
C(17)	−30(24)	3158(23)	3296(24)	90(12)
C(18)	533(19)	2796(18)	3846(18)	65(8)
C(19)	473(15)	6608(14)	−442(14)	38(6)
C(20)	−217(16)	6441(16)	19(16)	51(7)
C(21)	−879(17)	5782(16)	−175(16)	53(7)
C(22)	−792(18)	5304(16)	−885(16)	54(7)
C(23)	−127(18)	5437(17)	−1340(17)	56(7)
C(24)	536(17)	6100(15)	−1119(15)	46(7)
C(25)	968(14)	8066(13)	692(13)	29(5)
C(26)	241(21)	8538(18)	672(20)	76(9)
C(27)	24(23)	8877(22)	1412(21)	90(11)
C(28)	445(21)	8672(19)	2077(20)	74(9)
C(29)	1144(21)	8185(19)	2132(19)	73(9)
C(30)	1372(19)	7809(18)	1398(17)	66(8)
C(31)	842(16)	8135(14)	−1089(14)	37(6)
C(32)	−84(18)	8120(16)	−1359(16)	54(7)
C(33)	−397(20)	8601(17)	−1968(17)	62(8)
C(34)	293(19)	9041(17)	−2238(17)	61(8)
C(35)	1168(21)	9068(18)	−2018(18)	68(9)
C(36)	1492(18)	8601(15)	−1375(15)	48(7)

[a] Equivalent isotropic *U* defined as one-third of the trace of the orthogonalized $\mathbf{U}_{ij}$ tensor.

$$[Bu_4N]^+[ReOBr_4(H_2O)]^- \cdot PBu_3^n + \text{(HS, N, R)} \xrightarrow[0\ °C]{THF} -4Et_3NHBr$$

$$ReO(\eta^2\text{-}SC_5H_3N\text{-}3\text{-}R)_2(\eta^1\text{-}2\text{-}SC_5H_3N\text{-}3\text{-}R) \quad (2)$$

R = H (**7**)
R = $SiMe_3$ (**8**)

the ligand to rhenium ratio is 3:1. The infrared spectrum of **7** reveals a ν(ReO) at 962 cm^{-1} and features in the fingerprint region that are indicative of a coordinated pyridine-2-thiolate ligand. The room-temperature ^1H NMR spectrum for **7** exhibits all resonances associated with the 2-SC_5H_4N ligand coalesced into the baseline, indicating that a fluxional process involving

Table 4. Atomic Positional Parameters ($\times 10^4$) and Isotropic Temperature Factors (Å^2 $\times$ 10^3) for [ReO($SC_5H_4N_3$)$_3$] (**7**)

	x	*y*	*z*	*U*(eq)[a]
Re(1)	6443(1)	1054(1)	2742(1)	33(1)
S(1)	2589(1)	7564(2)	6096(2)	43(1)
S(2)	3750(2)	10178(2)	5856(2)	50(1)
S(3)	2660(2)	8457(2)	8498(2)	50(1)
O(1)	5027(5)	8551(5)	7624(4)	45(2)
N(1)	1157(7)	5782(7)	6100(6)	47(3)
N(2)	1968(6)	10121(6)	6530(5)	39(3)
N(3)	3771(6)	10323(6)	8335(5)	35(2)
C(1)	2159(8)	6288(7)	6645(7)	37(2)
C(2)	2887(9)	58O8(8)	7569(7)	47(2)
C(3)	2542(9)	4771(9)	7865(8)	59(3)
C(4)	1495(10)	4237(10)	7306(9)	66(3)
C(5)	835(10)	4764(10)	6419(8)	62(3)
C(6)	2332(8)	10655(8)	5828(7)	43(2)
C(7)	158O(9)	11494(9)	5180(8)	54(2)
C(8)	507(10)	11755(10)	5312(9)	67(3)
C(9)	137(11)	11217(9)	6058(9)	65(3)
C(10)	898(9)	10379(9)	6660(7)	53(2)
C(11)	3222(8)	9848(8)	8981(7)	39(2)
C(12)	3209(9)	10428(9)	9825(7)	53(2)
C(13)	3789(9)	11534(9)	10014(8)	53(2)
C(14)	4347(8)	11975(9)	9375(7)	54(3)
C(15)	4339(8)	11384(8)	8524(7)	44(2)

[a] Equivalent isotropic *U* defined as one-third of the trace of the orthogonalized $\mathbf{U}_{ij}$ tensor.

all three pyridine-2-thiolate ligands is occurring. The UV−visible spectrum of **7** consists of typical $\pi \rightarrow \pi^*$ transitions in the UV region, a ligand-to-metal charge transfer band at 365 nm (ϵ 6.3 $\times$ 10^3), and a d−d transition at 650 nm (ϵ 90).

In the case of [ReO(η^2-2-SC_5H_3N-3-$SiMe_3$)$_2$(η^1-2-SC_5H_3N-3-$SiMe_3$)] **(8)**, the yield of crystalline material was quite low (33%) due to the high solubility of this complex in typical organic solvents. The IR spectrum for **8** displays a strong ν(ReO) band at 966 cm^{-1} and a strong band at 841 cm^{-1} assigned to ν(Si−C). The ^{1}H NMR spectrum at room temperature exhibits broadened resonances both for the $-SiMe_3$ protons (0.44, 0.33, and 0.20 ppm) and for the aromatic pyridyl protons (8.68, 8.56, and 7.80 ppm). At 243 K, the three 2-S-C_5H_3N-3-$SiMe_3$ ligands are inequivalent, as indicated by three unique resonances for the $-SiMe_3$ protons at 0.20, 0.33, and 0.44 ppm. These data are consistent with the six-coordinate formulations shown in Chart 1. Due to electronic considerations, the pyridyl N-donor atoms generally occupy positions *trans* to the strongly π-bonding oxo ligands, thus minimizing competition between the oxo groups and the weakly π-donating thiolate S-donors for the rhenium t_{2g} orbitals.[39] Therefore, structures **8C** and **8D**, are unlikely. Of **8A** and **8B**, structure **8A** is most likely, by analogy to the solid-state structure of **7** (*vide infra*).

In order to evaluate the consequences of steric constraints on the structural chemistry of Re(V) thiolates, **3** was reacted with **5** under the same conditions used to prepare **7** and **8**. Similar workup conditions afforded light green materials which, upon dissolution in CH_2Cl_2, turned autumn-brown. Initially, it was thought that the CH_2Cl_2 solvent had not been dried thoroughly, but this color change occurred even with rigorously dried CH_2Cl_2 in a N_2-filled glovebox (P_{O_2} < 1 ppm). Therefore, two crystallization experiments were performed in which a portion of the crude product was recrystallized from hexanes to yield a green product, **9a**, and another portion of the crude product was recrystallized from CH_2Cl_2/CH_3OH to give the brown material **9**. The IR spectrum of **9a** displays no features in the 900−1000 cm^{-1} region, attributable to ν(ReO) but does exhibit a ν(SiC) band at 808 cm^{-1}. Further attempts to characterize **9a** by analytical, spectroscopic, and structural methods suggested reduction of the Re(V) by the thiolate to give [Re{SC_5H_2N-3,6-($SiMe_2Bu$)$_2$}$_3$]. The IR spectrum of **9**

Chart 1

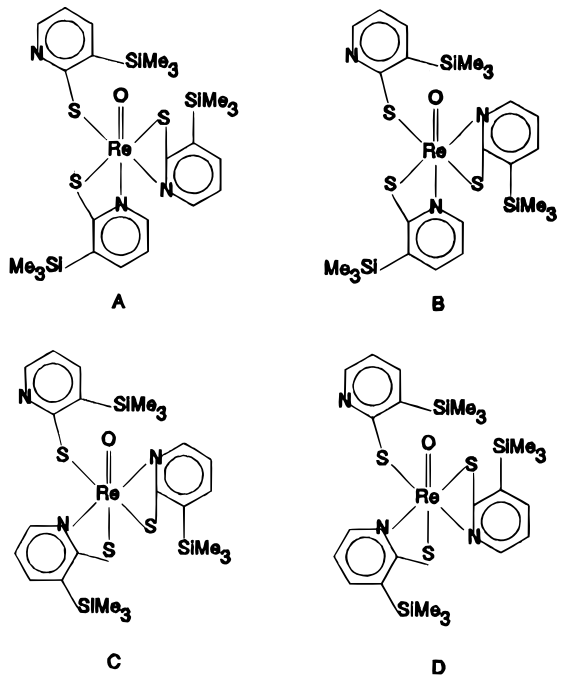

exhibits a strong band at 3439 cm^{-1} assigned to ν(O−H), a band at 952 cm^{-1} attributed to ν(Re═O), and the ν(Si−C) band at 806 cm^{-1}. The ^{1}H NMR spectrum displays two resonances each for the methyl (0.49 and 0.43 ppm) and *tert*-butyl groups (1.00 and 0.97 ppm) of the inequivalent $-SiMe_2Bu^t$ groups of the 2-SC_5H_2N-3,6-($SiMe_2Bu^t$)$_2$ ligands, indicating that the two 2-SC_5H_3N-3,6-($SiMe_2Bu^t$)$_2$ ligands are equivalent. The UV−visible spectrum of **9** exhibits intense ligand $\pi \rightarrow \pi^*$ and ligand-to-metal charge transfer bands between 245 and 400 nm (ϵ 8.1 $\times$ 10^3−9.8 $\times$ 10^3) and a d−d transition at 680 nm (ϵ 2.2 $\times$ 10^2). The identity of **9** as [ReO(OH)(η^2-2-SC_5H_2N-3,6-($SiMe_2Bu^t$)$_2$)$_2$] was confirmed by the X-ray crystal structure (*vide infra*).

The reactions of **1** with the rhenium(V) precursor [Re{$N_2CO(C_6H_5)$}$Cl_2(PPh_3)_2$] ("green chelate") were also investigated.[46] In a typical reaction, as illustrated by eq 3, addition

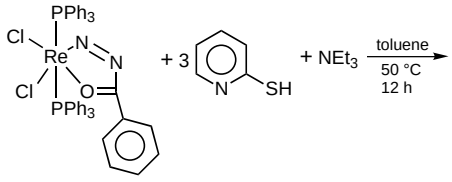

Re(η^1-$N_2CO(C_6H_5)$(η^2-2-SC_5H_4N)Cl(PPh_3)$_2$ (3)

10

of Et_3N to [Re({$N_2CO(C_6H_5)$}$Cl_2(PPh_3)_2$] and **1** in toluene at 50 °C led to the formation of a dark green solution from which the product [Re{η^1-$N_2CO(C_6H_5)$}(η^2-2-SC_5H_4N)Cl(PPh_3)$_2$] **(10)** crystallized in approximately 50% yield upon addition of toluene/hexanes. Compound **10** exhibits an IR spectrum with bands in the fingerprint region for the coordinated pyridine-2-thiolate ligand and a strong band at 1653 cm^{-1} assigned to ν(C═O), indicating that the chelating benzoyldiazenido ligand is monodentate through the α-nitrogen.[21] Elemental analysis and the ^{1}H NMR spectrum for **10** confirm that one 2-SC_5H_4N ligand is coordinated to rhenium. The ^{1}H NMR spectrum of **10** displays resonances in the aromatic region with integration consistent with a ratio of 2:1:1 for PPh_3:$PhC(O)N_2$:SC_5H_4N. The UV−visible spectrum consists of three intense bands at 233, 267, and 367 nm attributed to $\pi \rightarrow \pi^*$ transitions for the

Table 5. Atomic Positional Parameters ($\times 10^4$) and Isotropic Temperature Factors ($Å^2 \times 10^3$) for $[ReO(OH)(\eta^2\text{-}SC_5H_2N\text{-}3,6\text{-}(SiMe_2Bu^t)_2)_2]$ (**9**)

	x	*y*	*z*	*U*(eq)[a]
Re(1)	−31	9960	−23	28(1)
Re(1A)	664(1)	9465(1)	381(1)	17(1)
O(1)	−1288(12)	10838(11)	−300(10)	40(1)
O(1A)	2111(10)	8358(8)	943(7)	33(1)
O(2)	1654(9)	8900(8)	439(7)	25(1)
O(2A)	−2440(13)	10553(12)	−524(11)	53(1)
S(1)	247(4)	8857(3)	−1569(3)	41(1)
S(2)	−199(4)	10946(3)	1617(3)	45(1)
Si(1)	−1763(4)	6452(3)	−2073(3)	32(1)
Si(2)	−3398(4)	8393(3)	2877(3)	39(1)
Si(3)	2382(4)	12935(3)	2415(3)	30(1)
Si(4)	3948(4)	11027(3)	−2532(3)	39(1)
N(1)	−1612(11)	8357(9)	406(9)	69(1)
N(2)	2102(10)	11169(8)	−316(7)	57(1)
C(1)	−1121(9)	7903(8)	−454(8)	47(1)
C(2)	−2099(9)	7093(7)	−697(7)	28(1)
C(3)	−3523(11)	6580(10)	260(9)	67(1)
C(4)	−3699(11)	6899(10)	1304(8)	55(1)
C(5)	−2765(10)	7811(9)	1461(10)	63(1)
C(6)	−3979(11)	5894(10)	−2160(9)	60(1)
C(7)	−986(10)	7633(9)	−3329(8)	45(1)
C(8)	−262(11)	5146(8)	−2088(10)	64(1)
C(9)	−1146(12)	4060(9)	−1124(10)	74(1)
C(10)	1509(10)	5557(10)	−2016(9)	51(1)
C(11)	−44(11)	4784(9)	−3302(9)	53(1)
C(12)	−4178(10)	9980(8)	2598(7)	40(1)
C(13)	−1505(10)	8208(9)	3489(9)	52(1)
C(14)	−5219(10)	7492(8)	3956(8)	42(1)
C(15)	−6873(10)	7557(10)	3645(9)	53(1)
C(16)	−4808(12)	6190(9)	4365(9)	59(1)
C(17)	−5461(10)	8141(8)	5085(7)	40(1)
C(18)	1960(11)	11515(9)	812(8)	54(1)
C(19)	2780(10)	12477(7)	999(8)	44(1)
C(20)	3970(10)	12908(8)	102(8)	37(1)
C(21)	4368(10)	12500(8)	−970(10)	62(1)
C(22)	3462(10)	11638(8)	−1151(7)	43(1)
C(23)	1597(11)	11782(9)	3690(10)	68(1)
C(24)	4471(10)	13311(8)	2424(8)	39(1)
C(25)	778(9)	14222(8)	2453(6)	29(1)
C(26)	355(12)	14696(11)	3609(10)	82(1)
C(27)	1445(10)	15220(8)	1448(9)	44(1)
C(28)	−985(12)	13903(9)	2370(10)	68(1)
C(29)	1944(10)	11221(10)	−3028(10)	65(1)
C(30)	4695(11)	9465(9)	−2174(9)	58(1)
C(31)	5786(10)	11843(8)	−3735(8)	39(1)
C(32)	7552(10)	11738(10)	−3444(8)	68(1)
C(33)	5944(11)	11327(10)	−4725(9)	54(1)
C(34)	5245(11)	13236(8)	−3941(10)	65(1)

[a] Equivalent isotropic *U* defined as one-third of the trace of the orthogonalized $\mathbf{U}_{ij}$ tensor.

aromatic groups of the ligands and to ligand-to-metal charge transfer processes. The cyclic voltammetry displays a reversible one-electron oxidation at +0.27 V: $[Re\{N_2CO(C_6H_5)\}(SC_5H_4N)Cl(PPh_3)_2] \rightleftarrows [Re\{N_2CO(C_6H_5)\}(SC_5H_4N)Cl(PPh_3)_2]^+ + e^-$.

The reaction of $[ReO_2(C_5H_5N)_4]Cl$ with pyrimidine-2-thiol (**4**) in refluxing EtOH with Et_3N gave the lime green $[ReO(\eta^2\text{-}2\text{-}SC_4H_3N_2)_2(\eta^1\text{-}2\text{-}SC_4H_3N_2)]$ (**11**), in moderate yield. The compound is structurally analogous to compound **7** despite the different starting materials and method of preparation. Both contain thiolate coordinated in the η^1 mode, which is not an uncommon coordination mode for this ligand, as well as in the η^2-(N,S) mode. We were unsucessful in substituting the η^1 thiolate either with benzoylhydrazine or with thiolate **2**. The IR spectrum of **11** exhibits a strong band at 967 cm^{-1} attributed to ν(Re=O).

The filtrate from the synthesis of **11** also yielded $[Re(PPh_3)(C_5H_3N_2S)_3]$ (**12**) as a minor product of the reaction, which results from the presence of small amounts of $[ReOCl_2(OEt)(PPh_3)_2]$ in preparations of $[ReO_2(C_5H_5N)_4]Cl$. Unlike for **11**, oxo abstraction from the starting material, $[ReOCl_2(OEt)(PPh_3)_2]$, does occur in this instance, providing the unusual seven-coordinate Re(III) species **12**.

Table 6. Atomic Positional Parameters ($\times 10^4$) and Isotropic Temperature Factors ($Å^2 \times 10^3$) for $[Re(\eta^1\text{-}N_2CO(C_6H_5))(\eta^2\text{-}2\text{-}SC_5H_4N)Cl(PPh_3)_2]$ (**10**)

	x	*y*	*z*	*U*(eq)[a]
Re(1)	2260(1)	3007(1)	2027(1)	22(1)
Cl(1)	2373(2)	3928(2)	568(2)	30(1)
P(1)	1652(3)	1721(2)	1128(2)	27(1)
P(2)	2866(2)	4320(2)	2891(2)	25(1)
S(1)	1025(3)	2533(2)	3359(2)	35(1)
O(1)	4158(7)	1103(6)	3835(6)	149(4)
N(1)	3775(8)	2282(6)	2297(5)	28(3)
N(2)	4900(8)	1829(6)	2517(5)	30(3)
N(3)	304(7)	3827(6)	2059(5)	27(3)
C(1)	−137(9)	3469(7)	2842 (7)	31(2)
C(2)	−1365(11)	3862(9)	3141(8)	46(3)
C(3)	−2099(13)	4659(10)	2618(9)	57(3)
C(4)	−1644(11)	5019(9)	1803(8)	46(3)
C(5)	−449(10)	4598(8)	1529(7)	35(3)
C(6)	5066(10)	1241(8)	3348(7)	31(2)
C(7)	6376(9)	762(8)	3622(7)	33(2)
C(8)	7376(10)	1152(8)	3289(7)	39(3)
C(9)	8619(12)	679(10)	3556(9)	58(3)
C(10)	8815(12)	−165(9)	4162(8)	52(3)
C(11)	7849(11)	−547(9)	4487(8)	48(3)
C(12)	6606(10)	−98(8)	4230(7)	40(3)
C(13)	−18(9)	2048(7)	766(7)	29(2)
C(14)	−906(10)	1548(8)	1154(8)	43(3)
C(15)	−2176(11)	1880(9)	931(8)	49(3)
C(16)	−2568(11)	2696(9)	334(8)	47(3)
C(17)	−1713(10)	3207(8)	−63(8)	41(3)
C(18)	−436(10)	2867(8)	147(7)	39(3)
C(19)	1850(9)	452(7)	1707(7)	30(2)
C(20)	2274(10)	280(8)	2627(7)	35(2)
C(21)	2326(11)	−651(9)	3097(8)	45(3)
C(22)	1919(11)	−1400(9)	2646(8)	48(3)
C(23)	1552(11)	−1234(9)	1744(8)	46(3)
C(24)	1520(10)	−320(8)	1249(8)	45(3)
C(25)	2543(10)	1451(8)	57(7)	35(2)
C(26)	3810(10)	1412(8)	67(7)	38(3)
C(27)	4536(12)	1126(9)	−718(8)	51(3)
C(28)	3956(12)	908(10)	−1490(9)	58(3)
C(29)	2709(12)	953(9)	−1528(9)	56(3)
C(30)	1978(12)	1218(9)	−745(8)	48(3)
C(31)	3809(9)	3803(7)	3935(7)	27(2)
C(32)	5048(14)	3864(11)	4026(10)	68(4)
C(33)	5777(17)	3392(12)	4803(12)	87(5)
C(34)	5267(13)	2896(10)	5478(10)	62(4)
C(35)	4034(13)	2855(11)	5417(10)	67(4)
C(36)	3318(12)	3305(9)	4640(9)	55(3)
C(37)	3853(9)	5052(7)	2264(6)	24(2)
C(38)	379O(10)	6047(8)	2451(7)	37(3)
C(39)	4532(10)	6602(9)	1942(8)	42(3)
C(40)	5301(10)	6190(8)	1261(7)	37(3)
C(41)	5400(10)	5188(7)	1092(7)	33(2)
C(42)	4670(9)	4623(8)	1589(7)	31(2)
C(43)	1574(9)	5314(7)	3282(6)	27(2)
C(44)	1269(11)	5464(8)	4196(8)	44(3)
C(45)	225(13)	6262(10)	4391(10)	63(4)
C(46)	−416(12)	6880(10)	3701(9)	56(3)
C(47)	−122(12)	6726(9)	2792(9)	54(3)
C(48)	884(10)	5949(8)	2589(8)	40(3)

[a] Equivalent isotropic *U* defined as one-third of the trace of the orthogonalized $\mathbf{U}_{ij}$ tensor.

Description of the Structures. The structures of the molecular anions of $[Bu_4N][ReO(H_2O)Br_4]\cdot 2H_2O$ (**5**) and $[Bu_4N][ReO(OPPh_3)Br_4]$ (**6**) are illustrated in Figure 1. The structure of the anion of **5** consists of discrete mononuclear $[ReO(H_2O)Br_4]^-$ units with distorted octahedral geometry about the rhenium(V) site defined by the terminal oxo ligand, the aquo ligand, and four bromine atoms. The Re atom is located on a crystallographic 2-fold axis, as are the oxo and aquo ligands, necessitating a rigorously linear O(1)−Re−O(2) angle. The

Table 7. Atomic Positional Parameters ($\times 10^4$) and Isotropic Temperature Factors ($Å^2 \times 10^3$) for $[ReO(\eta^2\text{-}2\text{-}SC_4H_3N_2)_2(\eta^1\text{-}2\text{-}SC_4H_3N_2)]$ (**11**)

	x	*y*	*z*	*U*(eq)[a]
Re(1)	1347(1)	3257(1)	3626(1)	39(1)
S(1)	1882(7)	3135(4)	2798(2)	53(2)
S(2)	1073(8)	4238(4)	4294(2)	46(2)
S(3)	−1336(8)	2828(4)	3501(2)	47(2)
O(1)	2168(19)	2147(11)	3744(4)	59(6)
N(1)	802(19)	4655(11)	3219(5)	38(6)
N(2)	1190(26)	4949(11)	2432(5)	51(6)
N(3)	3434(19)	4169(12)	3744(5)	38(5)
N(4)	3927(25)	5269(14)	4354(5)	58(7)
N(5)	−2013(21)	3378(16)	4359(5)	60(7)
N(6)	−3679(27)	2162(13)	4016(6)	69(7)
C(1)	1263(29)	4374(14)	2796(7)	45(5)
C(2)	244(25)	5558(15)	3288(7)	40(5)
C(3)	142(26)	6195(17)	2929(7)	51(6)
C(4)	700(29)	5879(18)	2502(8)	64(7)
C(5)	3024(25)	4627(15)	4138(7)	41(5)
C(6)	4844(27)	4374(15)	3549(7)	47(6)
C(7)	5868(28)	5045(16)	3745(7)	56(6)
C(8)	5336(31)	5469(17)	4148(8)	62(7)
C(9)	−2453(26)	2772(14)	4020(6)	34(4)
C(10)	−2934(28)	3349(18)	4727(8)	66(7)
C(11)	−4287(28)	2704(16)	4747(8)	58(6)
C(12)	−4609(33)	2134(17)	4382(8)	68(8)

[a] Equivalent isotropic *U* defined as one-third of the trace of the orthogonalized $\mathbf{U}_{ij}$ tensor.

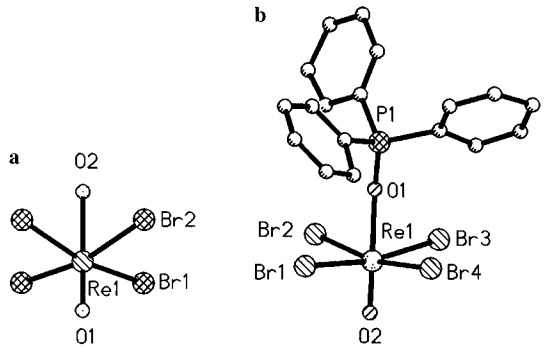

Figure 1. (a) View of the structure of the molecular anion of **5**, $[ReOBr_4(H_2O)]^-$. (b) View of the structure of the molecular anion of **6**, $[ReOBr_4(OPPh_3)]^-$.

metrical parameters are unexceptional. The Re−O(1) distance of 1.58(3) Å may be compared to distances of 1.57−1.66 Å in other examples of octahedral Re(V)−oxo species.[53,54] The Re−O(2) distance of 2.28(3) Å reflects a strong *trans* influence of the oxo ligands and the identity of O(2) as an aquo group.

The structure of **6** reveals the presence of two unique $(R_4N)^+$ cations and two crystallographically distinct $[ReO(OPPh_3)Br_4]^-$ anions. The structure of the anion of **6** is again distorted octahedral, with the oxo ligand, the four bromide donors, and the oxygen donor of the phosphine oxide defining the coordination sites. The Re−O (phosphine oxide) bond distance of 2.10(2) Å reflects the *trans* influence of the oxo ligand and may be compared to a value of 2.02 Å for Re−$OPPh_3$ in $[ReO(OPPh_3)(O(2)C_6Cl_4)_2]^-$.[54] Not unexpectedly, the Re−Br distances in **5** and **6** are essentially identical, and all other metrical parameters are similar.

In Re−thiolate species **7** and **9**−**12** exhibit a diverse structural chemistry. The structure of $[ReO(2\text{-}SC_5H_4N)_3]$ (**7**), shown in Figure 2, consists of neutral mononuclear units of distorted octahedral geometry. The rhenium center displays $\{ReOS_3N_2\}$ coordination through bonding to a terminal oxo ligand, two bidentate pyridinethiolate-*N*,*S* ligands, and a monodentate pyridinethiolate-*S* ligand. The thiolate donors assume *cis* orientations with respect to the terminal oxo ligand, a preferred geometry in oxorhenium−thiolate complexes which avoids competition of π-interacting oxo and thiolate ligands for the same metal t_{2g}-type orbitals. This arrangement of sulfur donors necessitates that one bidentate pyridinethiolate occupy the equatorial S_3N plane and that the second span the equatorial and axial positions. The N(2) donor is thus *trans* to the oxo ligand and exhibits a Re−N(2) distance of 2.242(6) Å, a significant elongation from that of 2.136(7) Å observed for Re−N(3). The

Table 8. Atomic Positional Parameters ($\times 10^4$) and Isotropic Temperature Factors ($Å^2 \times 10^3$) for $[Re(PPh_3)(\eta^2\text{-}2\text{-}SC_4H_3N_2)_3]$ (**12**)

	x	*y*	*z*	*U*(eq)[a]
Re(1)	10869(1)	1965(1)	1760(1)	23(1)
Cl(1)	10144(10)	2275(6)	−3266(5)	97(3)
Cl(2)	9891(12)	3161(9)	−1555(5)	135(5)
S(1)	11815(5)	3454(4)	1203(3)	31(2)
S(2)	12063(5)	−183(4)	2183(3)	33(2)
S(3)	9060(5)	925(4)	1484(3)	40(2)
P(1)	9384(5)	2944(4)	3009(3)	27(2)
N(1)	12253(14)	1431(11)	553(8)	23(5)
N(2)	13434(17)	2530(13)	−334(9)	39(6)
N(3)	12972(16)	1491(11)	2411(9)	32(5)
N(4)	14680(16)	−382(13)	3002(9)	37(6)
N(5)	8996(16)	2911(11)	969(8)	32(5)
N(6)	7080(19)	2314(13)	361(10)	45(6)
C(1)	7609(19)	4270(15)	2811(10)	31(4)
C(2)	7368(21)	5447(16)	3013(11)	40(4)
C(3)	5975(23)	6380(19)	2838(13)	52(5)
C(4)	4849(24)	6140(19)	2460(13)	53(5)
C(5)	5045(23)	4932(18)	2251(12)	48(5)
C(6)	6422(19)	4055(16)	2426(11)	36(4)
C(7)	5442(18)	2256(14)	3850(10)	29(4)
C(8)	7531(21)	2981(17)	4488(11)	42(5)
C(9)	6863(24)	2480(19)	5149(13)	54(5)
C(10)	7280(22)	1261(18)	5173(13)	49(5)
C(11)	8290(21)	519(18)	4547(12)	44(5)
C(12)	8923(19)	1022(15)	3878(11)	33(4)
C(13)	10565(18)	3498(14)	3672(10)	28(4)
C(14)	11071(22)	4410(18)	3396(13)	49(5)
C(15)	12071(22)	4699(18)	3859(12)	47(5)
C(16)	12773(25)	4046(19)	4556(13)	59(6)
C(17)	12223(25)	3119(20)	4869(14)	61(6)
C(18)	11240(21)	2862(17)	4399(12)	43(5)
C(19)	12737(17)	521(14)	−11(10)	26(4)
C(20)	13614(21)	601(17)	−769(12)	42(4)
C(21)	13929(22)	1578(17)	−874(12)	43(5)
C(22)	12641(18)	2395(14)	354(10)	26(4)
C(23)	13936(19)	2008(16)	2689(10)	34(4)
C(24)	15219(21)	1389(17)	3124(12)	41(4)
C(25)	15538(21)	221(17)	3247(12)	42(4)
C(26)	13410(18)	274(14)	2603(10)	28(4)
C(27)	8407(19)	3959(15)	583(10)	35(4)
C(28)	7182(21)	4199(18)	59(12)	44(5)
C(29)	6553(22)	3353(17)	−15(12)	47(5)
C(30)	8261(15)	2132(14)	867(10)	25(4)
C(31)	10833(33)	2042(26)	−2279(17)	90(8)

[a] Equivalent isotropic *U* defined as one-third of the trace of the orthogonalized $\mathbf{U}_{ij}$ tensor.

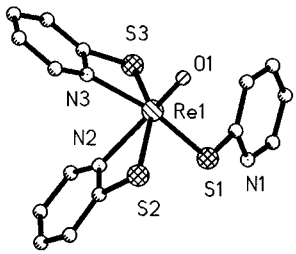

Figure 2. ORTEP representation of the structure of $[ReO(C_5H_4NS)_3]$ (**7**).

(53) Kettler, P. B.; Chang, Y.-D.; Zubieta, J.; Abrams, M. J. *Inorg. Chim. Acta* **1994**, *218*, 157.
(54) Edwards, C. F.; Griffith, W. P.; White, A. J. P.; Williams, D. J. *J. Chem. Soc., Dalton Trans.* **1992**, 957.

Table 9. Selected Bond Lengths (Å) and Angles (deg) for $[Bu_4N][ReOBr_4(H_2O)]\cdot 2H_2O$ (**5**)

Re(1)−Br(1)	2.499(10)	Re(1)−Br(2)	2.516(9)
Re(1)−O(1)	1.591(30)	Re(1)−O(2)	2.277(24)
Re(1)−Br(1A)	2.499(10)	Re(1)−Br(2A)	2.516(9)
Br(1)−Re(1)−Br(2)	90.7(3)	Br(1)−Re(1)−O(1)	97.5(3)
Br(2)−Re(1)−O(1)	97.7(2)	Br(1)−Re(1)−O(2)	82.5(3)
Br(2)−Re(1)−O(2)	82.3(2)	O(1)−Re(1)−O(1)	180.0(1)
Br(1)−Re(1)−Br(1A)	164.9(5)	Br(2)−Re(1)−Br(1A)	87.3
O(1)−Re(1)−Br(1A)	97.5(3)	O(2)−Re(1)−Br(1A)	82.5(3)
Br(1)−Re(1)−Br(2A)	87.3(3)	Br(2)−Re(1)−Br(2A)	164.7(4)
O(1)−Re(1)−Br(2A)	97.7(2)	O(2)−Re(1)−Br(2A)	82.3(2)
Br(1A)−Re(1)−Br(2A)	90.7(3)		

Table 10. Selected Bond Lengths (Å) and Angles (deg) for $[Bu_4N][ReOBr_4(OPPh_3)]$ (**6**)

Re(1)−Br(1)	2.518(3)	Re(1)−Br(2)	2.523(3)
Re(1)−Br(3)	2.538(3)	Re(1)−Br(4)	2.523(3)
Re(1)−O(1)	2.100(15)	Re(1)−O(2)	1.501(19)
Re(2)−Br(5)	2.545(3)	Re(2)−Br(6)	2.521(3)
Re(2)−Br(7)	2.520(3)	Re(2)−Br(8)	2.532(3)
Re(2)−O(3)	2.088(16)	Re(2)−O(4)	1.554(17)
O(1)−P(1)	1.517(17)	O(3)−P(2)	1.526(17)
P(1)−C(1)	1.793(21)	P(1)−C(7)	1.800(23)
P(1)−C(13)	1.811(24)	P(2)−C(19)	1.821(23)
P(2)−C(25)	1.833(23)	P(2)−C(31)	1.848(25)
Br(1)−Re(1)−Br(2)	89.3(1)	Br(1)−Re(1)−Br(3)	169.7(1)
Br(2)−Re(1)−Br(3)	88.1(1)	Br(1)−Re(1)−Br(4)	90.3(1)
Br(2)−Re(1)−Br(4)	167.4(1)	Br(3)−Re(1)−Br(4)	90.2(1)
Br(1)−Re(1)−O(1)	85.1(4)	Br(2)−Re(1)−O(1)	85.1(4)
Br(3)−Re(1)−O(1)	84.8(4)	Br(4)−Re(1)−O(1)	82.3(4)
Br(1)−Re(1)−O(2)	94.2(7)	Br(2)−Re(1)−O(2)	95.0(7)
Br(3)−Re(1)−O(2)	96.0(7)	Br(4)−Re(1)−O(2)	97.5(7)
O(1)−Re(1)−O(2)	179.3(3)	Br(5)−Re(2)−Br(6)	168.5(1)
Br(5)−Re(2)−Br(7)	90.3(1)	Br(6)−Re(2)−Br(7)	88.1(1)
Br(5)−Re(2)−Br(8)	90.5(1)	Br(6)−Re(2)−Br(8)	88.8(1)
Br(7)−Re(2)−Br(8)	168.7(1)	Br(5)−Re(2)−O(3)	84.6(4)
Br(6)−Re(2)−O(3)	84.0(4)	Br(7)−Re(2)−O(3)	83.9(4)
Br(8)−Re(2)−O(3)	85.0(4)	Br(5)−Re(2)−O(4)	92.9(5)
Br(6)−Re(2)−O(4)	98.6(3)	Br(7)−Re(2)−O(4)	96.3(6)
Br(8)−Re(2)−O(4)	94.9(6)	O(3)−Re(2)−O(4)	177.5(7)
Re(1)−O(1)−P(1)	165.4(9)	Re(2)−O(3)−P(2)	163.4(9)
O(1)−P(1)−C(1)	113.4(9)	O(1)−P(1)−C(7)	110.0(10)
		O(1)−P(1)−C(13)	111.9

third pyridine-2-thiol ligand adopts a monodentate coordination mode, presumably as a consequence of steric congestion about the $\{ReO\}^{3+}$ core of the complex. The ability of pyridinethiol ligands and derivatives to adopt a variety of coordination modes, within a single complex, is well-documented.[29−43,55] It is noteworthy that there are three distinct Re−S bond distances, reflecting both monodentate versus bidentate coordination modes and the geometries of the bidentate units. The Re−S(1) bond distance of 2.290(2) Å is significantly shorter than those observed for the Re−S bonds of the bidentate ligands, Re−S(2) and Re−S(3) of 2.481(3) Å and 2.350(3) Å, respectively. The shortening of this bond in **7** from the average Re−S bond distance of 2.341(3) Å in $[ReO(SPh)_4]^-$ [55,56] reflects the location of S(1) *trans* to the pyridine nitrogen donor N(3) in **7** in contrast to the situation in $[ReO(SPh)_4]^-$ where the thiolate sulfur atoms occupy positions *trans* to other π-interacting thiolate groups. The Re−S(3) distance of 2.350(3) Å is essentially identical to that observed for $[ReO(SPh)_4]^-$, while the significantly elongated Re−S(2) distance appears to reflect the requirements of the ligand to span equatorial−axial positions of the metal coordination sphere. Similar bond length trends are observed

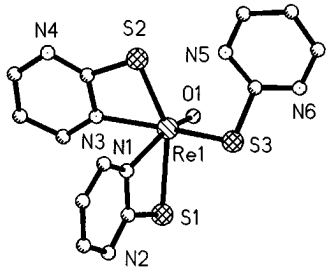

Figure 3. View of the structure of $[ReO(C_4H_3N_2S)_3]$ (**11**).

Table 11. Selected Bond lengths (Å) and Angles (deg) for $[ReO(SC_5H_4N_3)_3]$ (**7**)

Re(1)−S(1A)	2.290(2)	Re(1)−S(2A)	2.481(3)
Re(1)−S(3A)	2.350(3)	Re(1)−O(1A)	1.675(6)
Re(1)−N(2A)	2.242(6)	Re(1)−N(3A)	2.136(7)
S(1)−C(1)	1.782(9)	S(1)−Re(1A)	2.290(2)
S(2)−C(6)	1.712(10)	S(2)−Re(1A)	2.481(3)
S(3)−C(11)	1.762(9)	S(3)−Re(1A)	2.350(3)
O(1)−Re(1A)	1.675(6)	N(1)−C(1)	1.306(10)
N(1)−C(5)	1.333(14)	N(2)−C(6)	1.330(13)
N(2)−C(10)	1.335(14)	N(3)−C(11)	1.366(13)
S(1A)−Re(1)−S(2A)	88.0(1)	S(1A)−Re(1)−S(3A)	97.8(1)
S(2A)−Re(1)−S(3A)	152.8(1)	S(1A)−Re(1)−O(1A)	105.0(2)
S(2A)−Re(1)−O(1A)	93.7(2)	S(3A)−Re(1)−O(1A)	110.2(2)
S(1A)−Re(1)−N(2A)	86.2(2)	S(2A)−Re(1)−N(2A)	64.1(2)
S(3A)−Re(1)−N(2A)	89.7(2)	O(1A)−Re(1)−N(2A)	155.1(3)
S(1A)−Re(1)−N(3A)	158.5(2)	S(2A)−Re(1)−N(3A)	97.4(2)
S(3A)−Re(1)−N(3A)	68.3(2)	O(1A)−Re(1)−N(3A)	95.4(3)
N(2A)−Re(1)−N(3A)	77.7(2)	C(1)−S(1)−Re(1A)	112.9(3)
C(6)−S(2)−Re(1A)	82.9(3)	C(11)−S(3)−Re(1A)	83.0(3)
C(1)−N(1)−C(5)	118.2(8)	C(6)−N(2)−C(10)	121.1(7)
C(6)−N(2)−Re(1A)	102.1(6)	C(10)−N(2)−Re(1A)	136.7(7)
C(11)−N(3)−Re(1A)	101.8(5)		

Table 12. Selected Bond Lengths (Å) and Angles (deg) for $[ReO(OH)(\eta^2\text{-}SC_5H_2N\text{-}3,6\text{-}(SiMe_2Bu^t)_2)_2]$ (**9**)

Re(1)−O(1)	1.443 (11)	Re(1)−O(2)	1.898 (8)
Re(1)−S(1)	2.429 (3)	Re(1)−S(2)	2.464 (4)
Re(1)−N(1)	2.201 (10)	Re(1)−N(2)	2.189 (9)
S(1)−C(1)	1.760 (8)	S(2)−C(18)	1.849 (9)
O(1)−Re(1)−O(2)	174.5(6)	O(1)−Re(1)−S(1)	97.9(5)
O(2)−Re(1)−S(1)	87.5(3)	O(1)−Re(1)−S(2)	86.5(5)
O(2)−Re(1)−S(2)	88.2(3)	S(1)−Re(1)−S(2)	175.5(1)
O(1)−Re(1)−N(1)	99.0(3)	O(2)−Re(1)−N(1)	84.3(4)
O(2A)−Re(1)−N(1)	74.7(4)	S(1)−Re(1)−N(1)	64.7(3)
S(2)−Re(1)−N(1)	113.6(3)	O(1)−Re(1)−N(2)	97.9(5)
O(2)−Re(1)−N(2)	78.8(3)	S(1)−Re(1)−N(2)	113.2(2)
S(2)−Re(1)−N(2)	67.1(2)	N(1)−Re(1)−N(2)	163.1(3)
Re(1)−S(1)−C(1)	80.3(4)	Re(1)−S(2)−C(18)	85.4(4)
Re(1)−N(1)−C(1)	102.9(6)	Re(1)−N(1)−C(5)	131.6(9)
C(1)−N(1)−C(5)	124.9(10)	Re(1)−N(2)−C(18)	105.4(5)
Re(1)−N(2)−C(22)	140.4(8)	C(18)−N(2)−C(22)	114.1(8)
S(1)−C(1)−N(1)	111.3(7)		

in the structure of $[MoO(2\text{-}SC_4H_3N\text{-}3\text{-}SiMe_3)_2(NNR_2)]$,[58] where the Mo−S distances to the ligands confined to the equatoral plane and to that spanning the equatorial/axial positions are 2.432(1) and 2.514(1) Å, respectively. The consequences of spanning equatorial/equatorial or equatoral/axial sites are also manifest in the chelate angles S(3)−Re−N(3) and S(2)−Re−N(2) of 64.1(2) and 68.3(2)°, respectively.

The structural framework of the pyrimidine-2-thiol derivative $[ReO(2\text{-}SC_4H_3N_2)_3]$ (**11**) is essentially identical to that of **9**, as shown in Figure 3. The *trans* influence of the oxo ligand is again apparent in the lengthening of the Re−N(1) bond to 2.27-(2) Å, as compared to a value of 2.14(2) Å for Re−N(3). Once again, there are three distinct Re−S distances, reflecting the three different coordination modes adopted by the ligands.

(55) Block, E.; Obori-Okai, G.; Kang, H.; Zubieta, J. *Inorg. Chim. Acta* **1991**, *187*, 59 and references therein.
(56) McDonell, A. C.; Hambley, T. W.; Snow, M. R.; Wedd, A. G. *Aust. J. Chem.* **1983**, *36*, 253.
(57) Blower, P. J.; Dilworth, J. R.; Hutchinson, J. P.; Nicholson, T.; Zubieta, J. *J. Chem. Soc., Dalton Trans.* **1986**, 1339.
(58) Block, E.; Kang, H.; Zubieta, J. *Inorg. Chim. Acta* **1991,** *181*, 227.

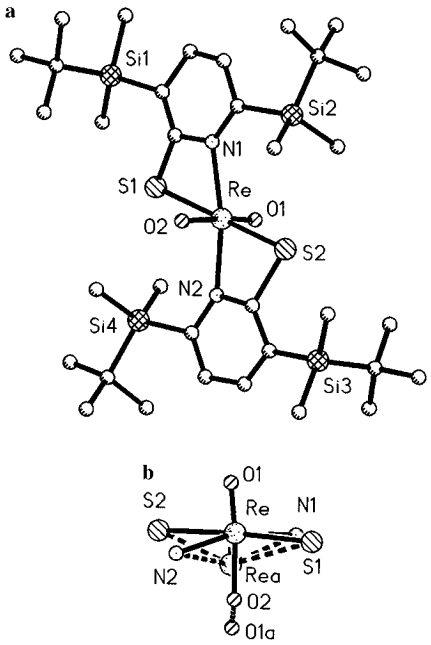

Figure 4. (a) Idealized structure of [ReO(OH)(η^2-SC_5H_2N-3,6-($SiMe_2Bu^t$)$_2$)$_2$] (**9**), showing the atom-labeling scheme. (b) View of the coordination sphere of **9**, illustrating the disorder of the {Re═O} grouping along the {ReO(OH)} vector.

Table 13. Selected Bond Lengths (Å) and Angles (deg) for [Re(η^1-$N_2CO(C_6H_5)$)(η^2-2- SC_5H_4N)Cl(PPh_3)$_2$] (**10**)

Re(1)−Cl(1)	2.402 (2)	Re(1)−P(1)	2.451 (3)
Re(1)−P(2)	2.452 (3)	Re(1)−S(1)	2.476 (3)
Re(1)−N(1)	1.751 (8)	Re(1)−N(3)	2.170 (7)
P(1)−C(13)	1.835 (10)	P(1)−C(19)	1.844 (10)
P(1)−C(25)	1.835 (11)	P(2)−C(31)	1.834 (9)
P(2)−C(37)	1.823 (10)	P(2)−C(43)	1.838 (9)
S(1) −C(1)	1.717 (9)	O(1)−C(6)	1.251 (14)
O(1)−C(7)	2.370 (13)	N(1)−N(2)	1.270 (11)
N(2)−C(6)	1.389 (12)	N(3)−C(1)	1.334 (13)
N(3)−C(5)	1.371 (12)		

Cl(1)−Re(1)−P(1)	86.6(1)	Cl(1)−Re(1)−P(1)	91.9(1)
P(1)−Re(1)−P(2)	178.6(1)	Cl(1)−Re(1)−S(1)	150.5(1)
P(1)−Re(1)−S(1)	90.2(1)	P(2)−Re(1)−S(1)	90.9(1)
Cl(1)−Re(1)−N(1)	107.7(3)	P(1)−Re(1)−N(1)	94.1(3)
P(2)−Re(1)−N(1)	86.4(3)	S(1)−Re(1)−N(1)	101.8(3)
Cl(1)−Re(1)−N(3)	86.1(2)	P(1)−Re(1)−N(3)	90.7(2)
P(2)−Re(1)−N(3)	89.1(2)	S(1) −Re(1)−N(3)	64.6(2)
N(1)−Re(1)−N(3)	165.6(3)	Re(1)−P(1)−C(13)	112.9(3)
Re(1)−P(1)−C(19)	116.8(3)	C(13)−P(1)−C(19)	103.7(5)
Re(1)−P(1)−C(25)	115.0(4)	C(13)−P(1)−C(25)	105.3(5)
C(19)−P(1)−C(25)	101.6(4)	Re(1)−P(2)−C(31)	112.3(3)
Re(1)−P(2)−C(37)	115.3(3)	C(31)−P(2)−C(37)	103.5(4)
Re(1)−P(2)−C(43)	116.8(3)	C(31)−P(2)−C(43)	105.7(4)
C(37)−P(2)−C(43)	101.7(4)	Re(1)−S(1)−C(1)	82.0(4)
C(6)−O(1)−C(7)	32.1(5)	Re(1)−N(1)−N(2)	174.8(8)
N(1)−N(2)−C(6)	116.8(8)	Re(1)−N(3)−C(1)	104.1(5)
Re(1)−N(3)−C(5)	135.7(7)		

The consequences of introducing sterically constraining substitutents on the ligands are revealed in the structure of [ReO(OH)(SC_5H_2N-3,6-$SiMe_2Bu^t$)$_2$] (**9**), shown in Figure 4a. The Re(V) center exhibits distorted octahedral geometry {ReO(2)S_2N_2} through coordination to an oxo ligand, to a hydroxo ligand, and to S,N-bidentate pyridinethiolate ligands. As illustrated in Figure 4b, the Re and oxygen sites are disordered about the normal to the S_2N_2 plane; consequently, the Re−O distances are somewhat unreliable. However, the Re−O(2) distance of 1.89(1) Å is significantly longer than Re(V)−oxo distances, which are generally observed in the 1.57−1.66 Å range, and considerably shorter than the Re(V)−aquo distances of 2.00−2.20 Å. Likewise, this distance is consistent with the expected value for a Re−OH group of 1.85−2.00 Å. The

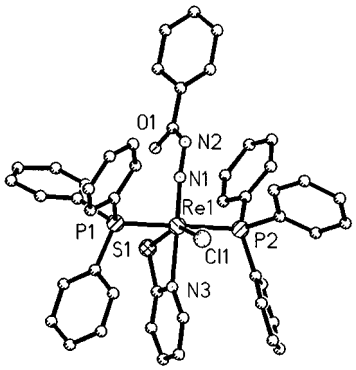

Figure 5. View of the structure of [Re(η^1-$N_2CO(C_6H_5)$)(η^2-2-SC_5H_4N)-Cl(PPh_3)$_2$] (**10**).

Table 14. Selected Bond Lengths (Å) and Angles (deg) for [ReO(η^2-2-$SC_4H_3N_2$)$_2$(η^1-2-$SC_4H_3N_2$)] (**11**)

Re(1)−S(1)	2.478(5)	Re(1)−S(2)	2.371(5)
Re(1)−S(3)	2.313(7)	Re(1)−O(1)	1.667(14)
Re(1)−N(1)	2.265(13)	Re(1)−N(3)	2.136(16)
S(1)−C(1)	1.734(20)	S(2)−C(5)	1.751(21)
S(3)−C(9)	1.783(19)	N(1)−C(1)	1.353(25)
N(1)−C(2)	1.307(25)	N(2)−C(1)	1.318(24)
N(2)−C(4)	1.324(29)	N(3)−C(5)	1.353(25)
N(3) −C(6)	1.324(27)	N(4)−C(5)	1.302(27)
N(4)−C(8)	1.337(32)	N(5)−C(9)	1.335(26)
N(5)−C(10)	1.322(28)	N(6)−C(9)	1.299(29)
N(6)−C(12)	1.322(32)	C(2)−C(3)	1.358(29)
C(3)−C(4)	1.401(31)	C(6)−C(7)	1.362(30)
C(7)−C(8)	1.384(30)	C(10)−C(11)	1.411(33)
C(11)−C(12)	1.342(33)		

S(1)−Re(1)−S(2)	150.0(2)	S(1)−Re(1)−S(3)	89.8(2)
S(2)−Re(1)−S(3)	100.3(2)	S(1)−Re(1)−O(1)	94.2(5)
S(2)−Re(1)−O(1)	111.1(5)	S(3)−Re(1)−O(1)	101.6(6)
S(1)−Re(1)−N(1)	64.6(4)	S(2)−Re(1)−N(1)	87.8(4)
S(3)−Re(1)−N(1)	86.0(4)	O(1)−Re(1)−N(1)	157.7(6)
S(1)−Re(1)−N(3)	93.0(4)	S(2)−Re(1)−N(3)	68.1(4)
S(3)−Re(1)−N(3)	159.5(4)	O(1)−Re(1)−N(3)	98.5(7)
N(1)−Re(1)−N(3)	76.9(6)	Re(1)−S(1)−C(1)	83.6(7)
Re(1)−S(2)−C(5)	82.0(7)	Re(1)−S(3)−C(9)	111.6(7)
Re(1)−N(1)−C(1)	101.5(11)	Re(1)−N(1)−C(2)	138.7(13)
C(1)−N(1)−C(2)	119.8(16)	C(1)−N(2)−C(4)	115.8(17)
Re(1)−N(3)−C(5)	101.3(12)	Re(1)−N(3)−C(6)	139.0(13)
C(5)−N(3)−C(6)	119.7(17)	C(5)−N(4)−C(8)	114.0(18)
C(9)−N(5)−C(lO)	116.0(19)	C(9)−N(6)−C(12)	117.5(19)
S(1)−C(1)−N(1)	110.2(14)	S(1)−C(1)−N(2)	124.9(15)

isolation of **9** under conditions similar to those yielding **7** or **11** with sterically unconstrained ligand types suggests that the steric influence of the ligand is a major structural determinant. On the other hand, electronic influences such as the β-silicon effect cannot be totally ruled out.

The structural chemistry of the class of Re−thiolate complexes may be further expanded by the introduction of triorganophosphine coligands, as demonstrated by the complexes [Re($N_2COC_6H_5$)(SC_5H_4N)Cl(PPh_3)$_2$] (**10**) and [Re(PPh_3)($SC_4H_3N_2$)$_3$] (**12**). As shown in Figure 5, the structure of **10** consists of discrete mononuclear units with the rhenium site in a distorted octahedral coordination geometry, [ReSClP_2N_2]. The coordination geometry about the rhenium center exhibits mutually *trans* phosphine ligands to minimize steric congestion. The equatorial plane is defined by the α-nitrogen donor of a monodentate benzoylhydrazido(3−) ligand, a chlorine atom, and the nitrogen and sulfur donors of a bidentate pyridine-2-thiolate ligand. The structure is related to that of the parent [Re($N_2COC_6H_5$)Cl_2(PPh_3)$_2$][21] by substitution of the N and S donors of the pyridine-2-thiolate ligand for a chlorine atom and the carbonyl oxygen of the benzoylhydrazido group of the parent compound. The Re−N(1) and N(1)−N(2) distances of 1.760(7) and 1.26(1) Å, respectively, are consistent with significant multiple-bond delocalization throughout the {Re−N−N} unit, as is the Re−

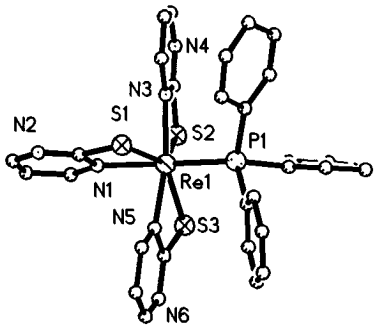

Figure 6. View of the structure of the seven-coordinate $[Re(PPh_3)(C_4H_3N_2S)_3]$ (**12**).

Table 15. Selected Bond Lengths (Å) and Angles (deg) for $[Re(PPh_3)(\eta^2\text{-}2\text{-}SC_4H_3N_2)_3]$ (**12**)

Re(1)−S(1)	2.401(3)	Re(1)−S(2)	2.504(4)
Re(1)−S(3)	2.497(6)	Re(1)−P(1)	2.349(4)
Re(1)−N(1)	2.157(11)	Re(1)−N(3)	2.138(15)
Re(1)−N(5)	2.148(13)	Cl(1)−C(31)	1.692(28)
Cl(2)−C(31)	1.692(27)	S(1)−C(22)	1.769(15)
S(2)−C(26)	1.709(20)	S(3)−C(30)	1.688(15)
P(1)−C(1)	1.851(15)	P(1)−C(7)	1.873(18)
P(1)−C(13)	1.854(19)	N(1)−C(19)	1.333(20)
N(1)−C(22)	1.365(24)	N(2)−C(21)	1.345(24)
N(2)−C(22)	1.297(21)	N(3)−C(23)	1.360(27)
N(3)−C(26)	1.401(21)	N(4)−C(25)	1.336(29)
N(4)−C(26)	1.337(20)	N(5)−C(27)	1.329(21)
N(5)−C(30)	1.365(26)	N(6)−C(29)	1.309(24)
N(6)−C(30)	1.343(24)		
S(1)−Re(1)−S(2)	136.3(1)	S(1)−Re(1)−S(3)	143.0(2)
S(2)−Re(1)−S(3)	70.3(2)	S(1)−Re(1)−P(1)	100.9(2)
S(2)−Re(1)−P(1)	103.9(1)	S(3)−Re(1)−P(1)	93.6(2)
S(1)−Re(1)−N(1)	67.2(4)	S(2)−Re(1)−N(1)	87.0(3)
S(3)−Re(1)−N(1)	95.1(4)	P(1)−Re(1)−N(1)	167.9(4)
S(1)−Re(1)−N(3)	80.2(4)	S(2)−Re(1)−N(3)	64.5(4)
S(3)−Re(1)−N(3)	134.1(4)	P(1)−Re(1)−N(3)	90.2(3)
N(1)−Re(1)−N(3)	89.9(5)	S(1)−Re(1)−N(5)	81.0(4)
S(2)−Re(1)−N(5)	132.8(4)	S(3)−Re(1)−N(5)	64.5(4)
P(1)−Re(1)−N(5)	91.9(3)	N(1)−Re(1)−N(5)	84.3(5)
N(3)−Re(1)−N(5)	161.2(S)	Re(1)−S(1)−C(22)	82.8(6)
Re(1)−S(2)−C(26)	83.2(5)	Re(1)−S(3)−C(30)	81.9(7)
Re(1)−P(1)−C(1)	114.5(5)	Re(1)−P(1)−C(13)	110.7(5)
Re(1)−P(1)−C(7)	125.5(5)		

N−N bond angle of 174.5(8)°. The metrical parameters associated with **10** are, in general, unexceptional, when compared to other examples of the $[Re(PPh_3)_2(N_2R)LL'L'']$ class of complexes.[21] The Re−S distance falls on the long end of the range of distances 2.26−2.50 Å observed for other examples of Re(V)−S(thiolate) complexes, suggesting that steric congestion may be responsible for some lengthening of the Re−S bond distance. The Re−N(3) distance of 2.171(7) Å does not appear to exhibit significant lenghtening as a consequence of the *trans* location relative to the strongly π-interacting benzoylhydrazido group. This observation is consistent with the negligible *trans* influence associated with hydrazido ligand type.

As shown in Figure 6, the structure of **12** represents a relatively rare example of a seven-coordinate rhenium complex of approximately pentagonal bipyramidal geometry. The axial positions of the coordination polyhedron are defined by the phosphorus donor of the triorganophosphine and the nitrogen of the bidentate pyrimidine-2-thiolate ligand which span the equatorial/axial positions. The pentagonal plane is generated by the sulfur and nitrogen donors of the remaining two pyrimidine-2-thiolate groups and the sulfur of the ligand spanning the equatorial/axial positions. In contrast to the observation in **7** and **11** that the Re−S distances associated with the ligand spanning the equatorial/axial positions are longer than those to the ligands involved in equatorial/equatorial interactions, the Re−S(1) distance of 2.401(5) Å is significantly shorter than the average of the Re−S(2) and Re−S(3) distances of 2.501(4) Å. The observation reflects important differences in the chemical types represented by complex **12**, and the Re(V) species **7**, **9**, and **11**. The coordination polyhedra are distinct, and the oxidation states of the Re centers are different, as are the identities of the coligands. While **7**, **9** and **11** possess a Re(V)-oxo core, **12** is an example of a Re(III) species. The *trans* influence of the oxo ligands in **7** and **11** serves to lenghten the Re−N bonds of the equatorial/axial ligand groups, a consequence of which may be a concomitant lengthening of the Re−S bond to the sulfur of the same ligand. The phosphine ligand of **12** clearly exerts no *trans* influence on the Re−N(1) bond, and the dominant influence in the lengthening of the Re−S(2) and the Re−S(3) distances appears to be steric congestion in the pentagonal plane.

Conclusions

Rhenium−thiolate chemistry is characterized by a diversity of structural types, which reflect the oxidation state of the rhenium, the nature of the coligands, and the introduction of steric constraints. Potentially chelating thiolate ligands of the pyridine-2-thiol and pyrimidine-2-thiol types appear to be particularly effective in the expansion of metal−thiolate chemistry in general as a consequence of robust coordination to metal centers and in view of the ability of the ligand classes to adopt a variety of coordination modes. This latter feature is manifest in the structures of $[ReO(SC_5H_4N)_3]$ (**7**) and $[ReO(SC_4H_3N_2)_3]$ (**11**), which exhibit both S,N-bidentate and S-monodentate binding modes of the ligands.

The consequences of introducing steric constriants are evident in the structure of $[ReO(OH)(2\text{-}SC_5H_2N\text{-}3,6\text{-}(SiMe_2Bu^t)_2)]$ (**9**), which accommodates two pyridinethiolate ligands rather than three as in the cases of **7** and **11**. The charge requirements of the Re(V) species are satisfied by coordination of a hydroxyl group.

The influence of coligands is exemplified in the structures of the $[Re(N_2COC_6H_5)(PPh_3)_2LL'L'']$ class of complexes and the variability of ligand type which may be introduced. Thiolates are effective as reducing reagents, a feature of the chemistry elaborated in the isolation of the Re(III) species $[Re(SC_4H_3N_2)_3(PPh_3)]$ (**12**) from a Re(V) precursor. The pentagonal bipyramidal geometry of **12** is relatively unusual for rhenium and demonstrates the structural versatility of the system.

Acknowledgment. We thank the Department of Energy Office of Health and Environmental Research for support of this work under Grant DE-FG02-93ERG1571.

Supporting Information Available: Tables giving details of data collection and refinement, bond distances and angles, anisotropic thermal parameters, and calculated hydrogen atom positions for **5**−**7** and **9**−**12** (52 pages). Ordering information is given on any current masthead page.

IC950881O